OPEN ACCESS

Original research

Duodenal *Anaerobutyricum soehngenii* infusion stimulates GLP-1 production, ameliorates glycaemic control and beneficially shapes the duodenal transcriptome in metabolic syndrome subjects: a randomised double-blind placebo-controlled cross-over study

Annefleur Koopen,[1] Julia Witjes,[1] Koen Wortelboer ,[1] Soumia Majait,[2] Andrei Prodan ,[3] Evgeni Levin,[1] Hilde Herrema,[3] Maaike Winkelmeijer,[3] Steven Aalvink,[4] Jacques J G H M Bergman ,[5] Stephan Havik,[3] Bolette Hartmann,[6] Han Levels,[3] Per-Olof Bergh,[7] Jamie van Son ,[1] Manon Balvers,[3] Diogo Mendes Bastos ,[1] Erik Stroes,[1] Albert K Groen,[1] Marcus Henricsson,[7] Ellis Marleen Kemper,[2] Jens Holst,[6] Christopher M Strauch,[8] Stanley L Hazen,[9] Fredrik Bäckhed,[7] Willem M De Vos ,[10] Max Nieuwdorp ,[1] Elena Rampanelli [3]

► Additional supplemental material is published online only. To view, please visit the journal online (http://dx.doi.org/10.1136/gutjnl-2020-323297).

For numbered affiliations see end of article.

Correspondence to
Dr Elena Rampanelli, Experimental Vascular Medicine, Amsterdam UMC Locatie AMC, Amsterdam, 1105 AZ North Holland, The Netherlands; e.rampanelli@amsterdamumc.nl

Received 6 October 2020
Accepted 9 October 2021
Published Online First 25 October 2021

To cite: Koopen A, Witjes J, Wortelboer K, *et al*. *Gut* 2022;**71**:1577–1587.

ABSTRACT

Objective Although gut dysbiosis is increasingly recognised as a pathophysiological component of metabolic syndrome (MetS), the role and mode of action of specific gut microbes in metabolic health remain elusive. Previously, we identified the commensal butyrogenic *Anaerobutyricum soehngenii* to be associated with improved insulin sensitivity in subjects with MetS. In this proof-of-concept study, we investigated the potential therapeutic effects of *A. soehngenii* L2-7 on systemic metabolic responses and duodenal transcriptome profiles in individuals with MetS.

Design In this randomised double-blind placebo-controlled cross-over study, 12 male subjects with MetS received duodenal infusions of *A. soehngenii*/ placebo and underwent duodenal biopsies, mixed meal tests (6 hours postinfusion) and 24-hour continuous glucose monitoring.

Results *A. soehngenii* treatment provoked a markedly increased postprandial excursion of the insulinotropic hormone glucagon-like peptide 1 (GLP-1) and an elevation of plasma secondary bile acids, which were positively associated with GLP-1 levels. Moreover, *A. soehngenii* treatment robustly shaped the duodenal expression of 73 genes, with the highest fold induction in the expression of regenerating islet-protein 1B (*REG1B*)-encoding gene. Strikingly, duodenal *REG1B* expression positively correlated with GLP-1 levels and negatively correlated with peripheral glucose variability, which was significantly diminished in the 24 hours following *A. soehngenii* intake. Mechanistically, Reg1B expression is induced upon sensing butyrate or bacterial peptidoglycan. Importantly, *A. soehngenii* duodenal administration was safe and well tolerated.

Conclusions A single dose of *A. soehngenii* improves peripheral glycaemic control within 24 hours; it specifically stimulates intestinal GLP-1 production and *REG1B* expression. Further studies are needed to delineate the specific pathways involved in REG1B induction and function in insulin sensitivity.

Trial registration number NTR-NL6630.

Significance of this study

What is already known on this subject?

⇒ Intestinal microbiota shapes host metabolic fitness and gut dysbiosis is associated with metabolic disorders.

⇒ Intestinal *Anaerobutyricum soehngenii* levels associate with enhanced insulin sensitivity in subjects with metabolic syndrome (MetS).

⇒ Oral *A. soehngenii* L2-7 supplementation improves insulin resistance in diabetic obese db/db mice.

INTRODUCTION

Along with lifestyle, diet and visceral obesity, the gut microbiota constitutes an important modulator of metabolic heath.[1] Accumulating evidence has now established that intestinal microbiota–diet–host interactions shape host metabolic homeostasis[2–4]; particularly, an unbalanced gut microbiome is increasingly recognised as an important risk factor for metabolic disorders, such as obesity, insulin resistance and type 2 diabetes (T2D).[3–5] In the pursuit of novel therapeutic insight for the rising cardiometabolic disease burden, the development of culture-independent approaches using high-throughput

Significance of this study

What are the new findings?

⇒ A single-dose of duodenal infusion containing *A. soehngenii* L2-7 is sufficient to improve peripheral glucose metabolism in human MetS.
⇒ *A. soehngenii* L2-7 stimulates the secretion of the incretin hormone GLP-1, which is reported to act on both insulin secretion and sensitivity.
⇒ Treatment with *A. soehngenii* specifically upregulates duodenal expression of regenerating islet-protein (*REG*)*1A/B*.
⇒ Duodenal *REG1B* expression associates with improved glycaemic control and GLP-1 levels.
⇒ Delivery of *A. soehngenii* into small intestine is shown, for the first time, to be safe and well tolerated.

How might it impact on clinical practice in the foreseeable future?

⇒ This study provides new insights into how intestinal microbes can affect host metabolism via duodenal signals.
⇒ Duodenal engraftment by multiple *A. soehngenii* administrations may be a novel treatment against insulin resistance in obesity and type 2 diabetes.

sequencing has tremendously advanced our knowledge of the microbial signatures of obesity and T2D.[6] General traits of obesogenic microbiota include a decline in faecal microbial community diversity, constriction of species richness and deprivation in short-chain fatty acid (SCFA)-producing microbes.[7 8] Nonetheless, the exact mechanisms by which specific bacterial strains regulate metabolic functions and influence the pathophysiology of metabolic disorders in humans are still poorly understood.

In an attempt to move from association to causality, we previously conducted repetitive faecal microbiota transplantations (FMTs) in humans to gain insights into the microbiome-derived effects on glucose and lipid metabolism. We proved that transfer of healthy microbiota from lean donors into patients with metabolic syndrome (MetS) improved their peripheral insulin sensitivity[3 4] and discovered that the latter was associated with increased relative abundance of *Anaerobutyricum* spp, including *Anaerobutyricum soehngenii*, in the small intestine (SI) following lean donor FMTs.[3]

A. soehngenii (formerly classified *Eubacterium hallii*) strain L2-7 is an anaerobic Gram-positive, catalase-negative bacterium belonging to the Lachnospiraceae family of the phylum Firmicutes.[9] This strain is capable of converting sugars as well as lactate and acetate into the SCFA butyrate,[10] which was shown to exert beneficial effects on glucose metabolism in obese mice and lean humans,[11 12] thus underscoring a potential therapeutic benefit of intestinal *A. soehngenii*. We previously described the efficacy of oral *A. soehngenii* L2-7 supplementation in improving insulin resistance and energy expenditure in diabetic and obese db/db mice.[13] Moreover, in a phase I/II safety and dose-finding trial, we showed that daily oral intake of *A. soehngenii* L2-7 for 4 weeks is safe and well tolerated and disclosed a positive correlation between faecal *A. soehngenii* L2-7 abundance and whole-body glucose rate of disposal.[14] However, a major disadvantage of oral administration of bacterial strains is the loss of viability due to contact with oxygen and stomach acid. Therefore, in the present study, duodenal tube infusion was chosen to bypass this issue and, hence, maximise the therapeutic potential by delivering viable bacteria directly into the SI, the first anatomical site with a central role in glucosensing, regulation of peripheral insulin sensitivity/secretion and glucose homeostasis.[15]

In this regard, within the intestinal milieu, SI enteroendocrine cells act as 'chemo sensors' of diet-derived and microbiota-derived metabolites, such as butyrate, and can regulate host glucose metabolism by secreting a variety of hormones, such as the incretin glucagon-like peptide-1 (GLP-1), which in turn enhances both insulin secretion and sensitivity.[15–17] However, the impact of single bacterial strains on the human enteroendocrine system remains elusive.

We therefore performed a randomised double-blind placebo-controlled cross-over trial to determine the localised and systemic effects of a single duodenal infusion of *A. soehngenii* L2-7 in male subjects with MetS. Our primary objective was to characterise the immediate changes induced by *A. soehngenii* L2-7 in the SI transcriptomic profile (6 hours postinfusion). Secondary objectives consisted in investigating the effects of *A. soehngenii* L2-7 on circulating (postprandial) incretins, faecal SCFA rates as well as gut microbiota composition.

Table 1 Baseline characteristics at screening

	Screening (n=12)
Male gender (%)	100
Age (years)	64(56 – 67)
Waist circumference (cm)	120(115 – 127)
Weight (kg)	113.6 (99.5–122.2)
BMI (kg/m^2)	35.9 (32.3–37.9)
Blood pressure: systolic (mm Hg)	146(136 – 159)
Blood pressure: diastolic (mm Hg)	95(86 – 98)
Fasting glucose (mmol/L)	5.8 (5.5–6.4]
Insulin (pmol/L)	82(66 – 116)
HOMA-IR	3.3 (2.3–4.0]
HbA1c (mmol/mol)	37(36–38)
Cholesterol: total (mmol/L)	5.04 (4.87–6.47)
Cholesterol: HDL (mmol/L)	1.25 (1.03–1.37)
Cholesterol: LDL (mmol/L)	3.12 (2.90–4.02)
Cholesterol: triglycerides (mmol/L)	1.74 (1.27–2.30)
Creatinine (µmol/L)	88(81 -95)
AST (U/L)	26(24–30)
ALT (U/L)	31(23–37)
AP (U/L)	77(63 – 92)
yGT (U/L)	35(22 – 66)
CRP (mg/mL)	3.1 (1.7–5.6)
Leucocytes (10^9/L)	6.1 (5.3–6.9)

All parameters were measured at fasted state. Values expressed as medians and IQRs.
ALT, alanine transaminase; AP, alkaline phosphatase; AST, aspartate transaminase; BMI, body mass index; CRP, C reactive protein; γGT, gamma-glutamyltransferase; HbA1c, glycated haemoglobin; HDL, high-density lipoprotein; HOMA-IR, homeostatic model assessment of insulin resistance; LDL, low-density lipoprotein.

RESULTS

Baseline characteristics and safety parameters

We included 15 Caucasian treatment-naïve men with MetS. During the trial, three subjects were excluded (two subjects refrained from participation after the screening due to personal reasons, and one subject was excluded because of antibiotic use), and thus 12 subjects were left for primary endpoint analyses. Baseline characteristics are presented in table 1. Participants were randomised to receive either 10% glycerol infusion (placebo,

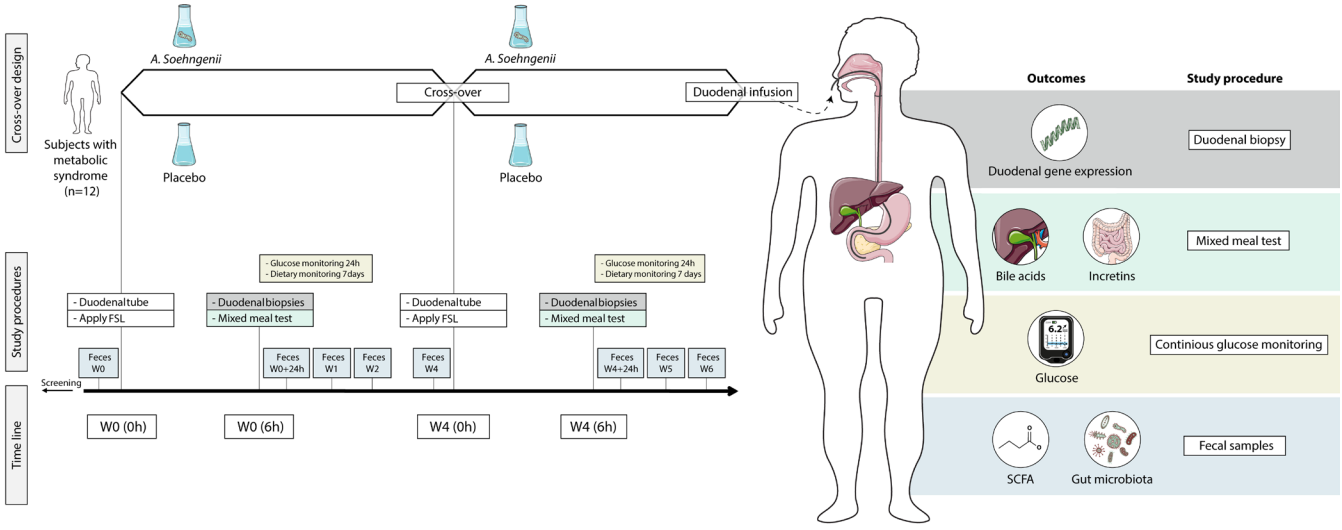

Figure 1 Study overview. Schematic representation of the study design showing the time points of interventions and of biological samplings: all 12 subjects received placebo (10% glycerol in PBS) or treatment (*Anaerobutyricum soehngenii* L2-7) at week 0 or 4 (time of intervention cross-over). FSL, FreeStyle Libre System; SCFA, short-chain fatty acid.

n=6) or 10^{11} cells of *A. soehngenii* L2-7 in 10% glycerol (treatment, n=6) as first intervention, and switch to treatment/placebo 4 weeks later (figure 1). Both infusions were well tolerated and no (severe) adverse events occurred during the entire study. Safety laboratory parameters (inflammatory, kidney and liver parameters) were all stable during the study. Energy and macronutrient intake did not differ in the week after *A. soehngenii* L2-7 or placebo administration (online supplemental table S1). We also observed no differences in body weight, blood pressure, glucose, insulin, homeostatic model assessment of insulin resistance (HOMA-IR) or cholesterol levels between placebo and *A. soehngenii* L2-7 treatments (online supplemental table S1).

Single-dose of *A. soehngenii* L2-7 has no impact on microbiota richness/diversity nor fecal SCFA

To discern the impact of *A. soehngenii* L2-7 infusion on gut microbial communities, 16S rRNA gene amplicon sequencing was performed using faecal DNA extracted from stool samples collected at baseline, 1 day, and 1 and 2 weeks after interventions. A single infusion of *A. soehngenii* L2-7 did not affect gut microbiota composition or alpha-diversity (Shannon index) either in the short term (24 hours) or long term (2 weeks) after intervention (figure 2A,B). Similarly, the abundance of *A. soehngenii* L2-7 in faecal samples, assessed by qPCR, was not durably altered over time (online supplemental figure S1). Notably, these data exclude microbiota-mediated carry-over effects at the time of cross-over (4 weeks after first intervention). Duodenal *A. soehngenii* L2-7 levels were below minimal detection rates, indicating that administered *A. soehngenii* L2-7 is not colonising the SI but rather transiting through the intestinal tract.

Given the capacity of *A. soehngenii* to produce butyrate (from sugars and lactate/acetate) and propionate (from 1,2-propanediol),[10 18 19] SCFAs (butyrate, acetate and propionate) were measured in faecal samples taken at baseline and 24 hours after duodenal infusion. Surprisingly, glycerol placebo intervention significantly decreased the levels of butyrate and acetate (p=0.02 and p=0.01, respectively), whereas faecal SCFA remained stable on *A. soehngenii* L2-7 delivery (online supplemental figure S2A–C), indicating that the vehicle glycerol-containing solution inhibits SCFA production. However, when comparing the intervention-induced changes in SCFA concentrations within the first 24 hours, no significant differences were found between placebo and treatment groups (figure 2C–E). Nonetheless, fold-change values of butyrate tended to be higher following *A. soehngenii* L2-7 feeding (p=0.06, figure 2C).

A. soehngenii L2-7 intake increases postprandial GLP-1 response and reduces the extent of glucose variability

To establish the immediate metabolic effects of *A. soehngenii* L2-7 intake, a standardised mixed meal test (MMT) was performed in all participants 6 hours postinterventions and the excursion of incretins, glucose, insulin and triglycerides was followed over 120 min. A significant increase in postprandial plasma GLP-1 levels was observed upon *A. soehngenii* L2-7 treatment (figure 3A,B; p=0.021). In line with this, during the first 24 hours, glucose excursions, determined as median absolute deviations (MADs) of continuous glucose measurements by FreeStyle Libre technology, were significantly diminished after *A. soehngenii* L2-7 intake compared with placebo infusion (figure 3C, p=0.045). In contrast, postprandial circulating levels of gastric inhibitory polypeptide (GIP), glucose, insulin and triglycerides were comparable between the two interventions (online supplemental figure S3A–D). Given the higher faecal butyrate levels 24 hours post-*A. soehngenii* infusion, we assessed the concentrations of plasma SCFA at the end of the MMT; however, no significant differences in butyrate, acetate or propionate levels were observed between placebo and treatment intervention-groups (online supplemental figure S4A–C).

Since the genome of *A. soehngenii* L2-7 strain includes genes encoding a bile acid (BA) sodium symporter (EHLA_2286) and BA hydrolases (EHLA_1602 and EHLA_2245),[20 21] we investigated the effects of *A. soehngenii* L2-7 on secondary BA. Although borderline significant (p=0.06), *A. soehngenii* L2-7 infusion augmented the postprandial excursions of secondary BA (figure 3D). Notably, the postprandial levels of the secondary BA taurodeoxycholic acid (TDCA), taurolithocholic acid (TLCA) and glycodeoxycholic acid (GDCA) positively correlated with the GLP-1 postprandial excursion rate, whereas iso-ursodeoxycholic acid (isoUDCA) rates were associated with GLP-1 concentrations at 6 hours postinfusion (figure 3E).

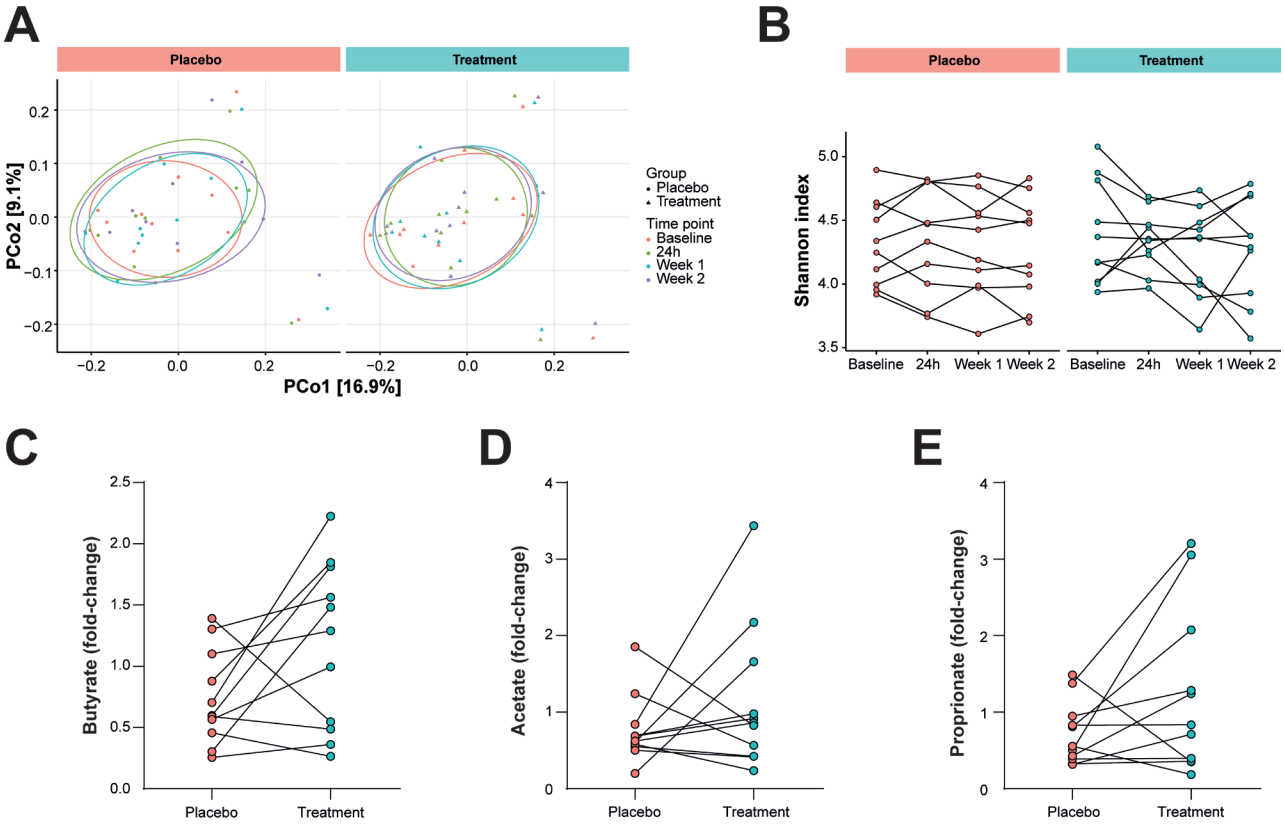

Figure 2 Microbiota composition and faecal SCFA. (A) Principal coordinate analysis plot on the unweighted UniFrac distances showing the clusters of 16S rRNA sequences. (B) Alpha diversity (Shannon Index) in faecal microbiota composition in stool samples collected at baseline, 1 day, and 1 and 2 weeks after placebo/treatment intervention. (C) Faecal levels of butyrate (p=0.06), (D) acetate and (E) propionate shown as fold change of concentrations (nmol/mg dried faeces weight) obtained 1 day after intervention versus baseline. SCFA, short-chain fatty acid.

In light of the positive effects of *A. soehngenii* L2-7 on GLP-1 and BA plasma concentrations, we subsequently questioned whether the observed systemic outcomes were linked to differential expression of the butyrate and BA receptors in SI. Indeed, both butyrate and BA may act as GLP-1 secretagogues on intestinal L cells by binding the transmembrane receptors G protein-coupled receptor 43 (GPR43) and Takeda G protein-coupled receptor 5 (TGR5), respectively,[22 23] whereas activation of the nuclear BA farnesoid X receptor (FXR) inhibits GLP-1 secretion.[24 25] Gene expression of *GPR43*, *TGR5*, *FXR* and of the FXR target genes *OSTa* and *FGF19* [26 27] was analysed in duodenal biopsies taken at 6 hours postinfusion (figure 4A–E). Gene expression of *GPR43*, *TGR5* and *FGF19* was comparable between placebo and treatment (median fold change equal to 1.3, 1.1 and 0.9, respectively) (figure 4A,B,E). Instead, upon *A. soehngenii* L2-7 intake, the transcript levels of *OSTa* were significantly decreased, while *FXR* expression tended to be lower (median fold change equal to 0.8 and 0.86, respectively) (figure 4C,D), hinting to a reduced FXR activity.

A. soehngenii L2-7 significantly impacts duodenal gene expression with a remarkable upregulation of regenerating islet-protein (*REG*)*1B* expression

To obtain an unbiased and in-depth snapshot of the intestinal transcriptome upon placebo/treatment infusions, we employed RNA sequencing (RNAseq) technology using RNA isolated from duodenum biopsies. The RNAseq data set analysis shows that a single dose of *A. soehngenii* L2-7 is sufficient to substantially change the transcriptomic profile of duodenal mucosa as early as 6 hours after intake. Indeed, using the digital gene expression (DGE) analysis pipelines Sleuth, EdgeR and DESeq2, we found respectively 380, 323 and 217 genes significantly upregulated or downregulated by *A. soehngenii* L2-7 intake (figure 5A). Only the genes with significant adjusted p values in all three statistical packages were retained, resulting in a total of 73 differentially expressed genes between placebo and treatment (figure 5B). Among these genes, *REG1B*, *LCN2* and *SLC6A14*, showed an upregulation above two log2(fold-change) after *A. soehngenii* treatment, whereas *DISP2* was the most downregulated gene (−1 log2(fold-change)) as compared with placebo (figure 5C). Overall, the most remarkable effect was the *A. soehngenii*-induced expression of *REG1B*, which encodes for the regenerating islet-derived 1 beta protein (figure 5C,D). Originally discovered in pancreatic calculi, Reg family members 1–4 are small secreted proteins that have been reported to promote proliferation, β-cell mass expansion and exert antidiabetogenic activities.[28–30] We, therefore, further studied the gene and protein expression of Reg1B in SI biopsies after placebo/treatment interventions. By quantitative PCR (qPCR), we validated the RNAseq findings on *REG1B* expression and found that the expression of the closely related *REG1A* gene was also strongly upregulated in response to *A. soehngenii* treatment (figure 5E,F and online supplemental figure S5A), whereas the transcript levels of *REG3A*, *REG3G* and *REG4* were not significantly upregulated by *A. soehngenii* L2-7 infusion (online supplemental figure S5B–D). We next questioned whether the treatment-mediated intestinal alterations are linked to systemic responses. Strikingly, an inverse correlation was found between the duodenal expression of the most

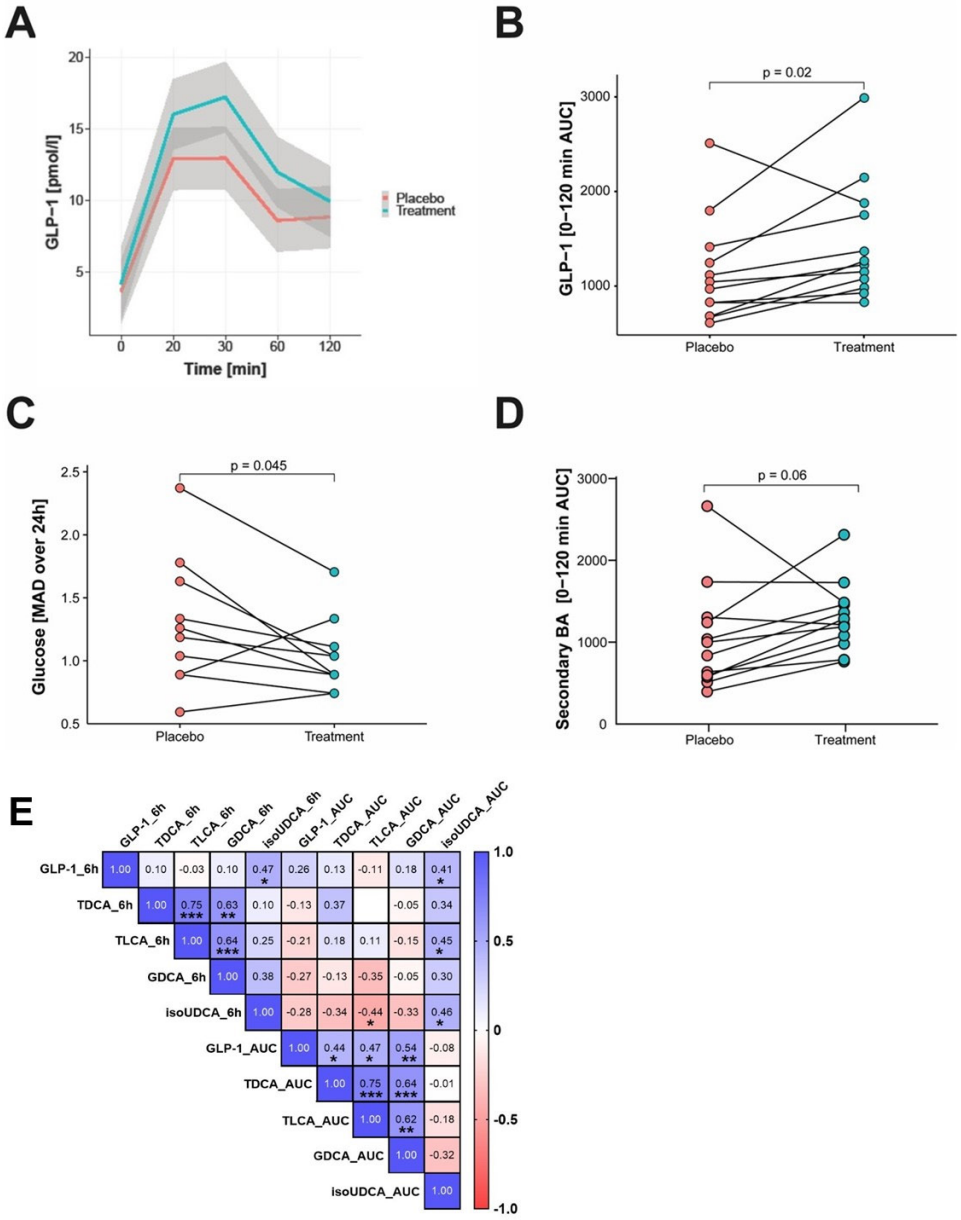

Figure 3 GLP-1, glucose and BA metabolism. (A) Plasma GLP-1 levels (pmol/L) at 0, 20, 30 and 120 min during MMT. (B) Plasma GLP-1 levels during MMT as total AUC. (C) MAD of continuous glucose measurements over the first 24 hours after placebo/treatment intervention. (D) Total secondary BA plasma levels during MMT, shown as the sum of AUCs of TOMCA, TUDCA, TDCA, TUDCA, TLCA, GHDCA, GDCA, GUDCA, GlcA, omcA, DCA, UDCA, LCA, HDCA, MuroCA and IsoUDCA. (E) Correlation heatmap showing the Spearman's r rank correlation coefficients and statistically significant correlations. *P≤0.05, **P≤0.01, ***P≤0.001 between BA and GLP-1 levels 6 hours postinfusion (6 hours) or during the MMT (AUC). MMT, mixed meal test; AUC, area under the curve; MAD, median absolute deviation; BA, bile acid; GLP-1, glucagon-like peptide 1; GDCA, glycodeoxycholic acid; TDCA, taurodeoxycholic acid; TLCA, taurolithocholic acid; isoUDCA; iso-ursodeoxycholic acid.

upregulated genes *REG1B*, *LCN2* and *SLC6A14* and systemic glucose variability (MAD), monitored continuously in the first 24 hours (figure 5G). In addition, duodenal *REG1B* levels were positively associated with the expression rates of *LCN2* and *SLC6A14*, and most importantly with the plasma concentrations of GLP1, underscoring systemic favourable effects of this single-bacterial strain intervention (figure 5G,H).

Subsequently, we investigated the intestinal expression and localisation of Reg1B and Reg1A proteins by western blotting and immunohistochemistry (IHC) in small intestinal tissues. At protein level, the mean expression of Reg1B and Reg1A within the duodenal mucosa trended toward higher expression after treatment, although not significant compared with placebo (figure 6A–C and online supplemental figure S5E–G). This inconsistency with gene expression rates is likely due to the fact that Reg proteins are secreted molecules. Immunostaining for Reg1B (performed with two different antibodies) showed a strong expression at the base of the crypts, where also stem cells and Paneth cells are located, and a milder staining throughout the villi and in the area delimiting vacuolated cells (figure 6D and online supplemental figure S5H). Comparing the IHC staining for Reg1B and Reg1A, at the same antibody concentrations, revealed that both proteins localize at the duodenal crypt bases, with Reg1B being more prominently expressed both in the crypt and villi compartments (online supplemental figure S5H). Since Reg1A and Reg1B belong to the same protein family

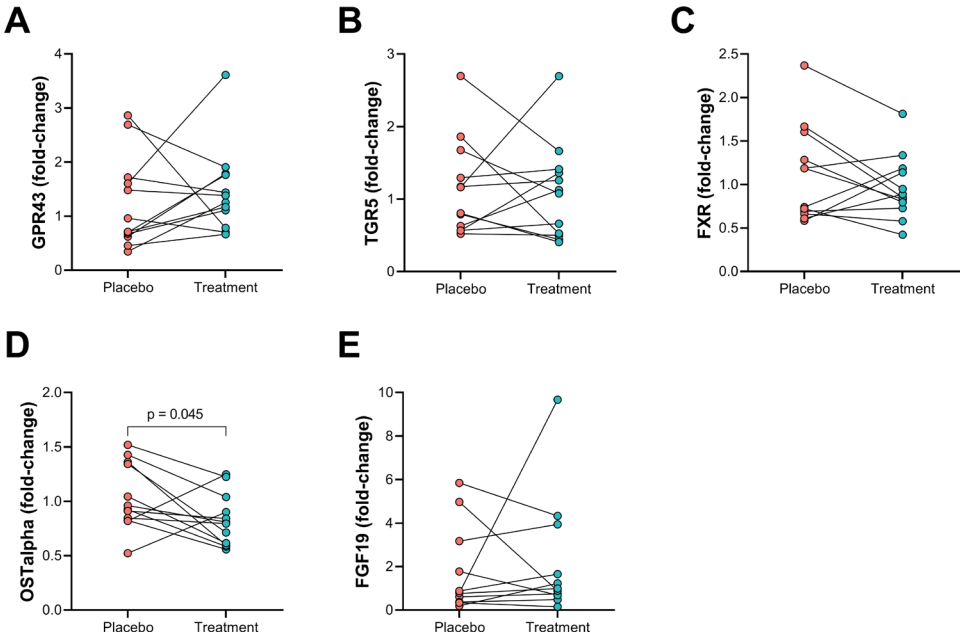

Figure 4 Duodenal gene expression. Gene expression measured by quantitative in duodenal biopsies of (A) *GPR43*, (B) *TGR5*, (C) *FXR*, (D) *OSTalpha* and (E) *FGF19*. Data showing the relative gene expression (to placebo) using the $2^{-\Delta\Delta Ct}$ method.

and are highly similar proteins of almost equal size, we excluded cross-reactivity of anti-Reg1A/B antibodies by using recombinant human Reg1B and Reg1A proteins in western blotting assays, as performed by Zheng *et al*.[31] The antibodies directed against Reg1B did not recognise Reg1A and vice versa (online supplemental figure S5I,K).

To further unravel the nature of the cell types expressing REG1B within crypt-villus units, we performed a triple-staining to visualize Reg1B (red), lysozyme (yellow, Paneth cell marker), and mucins (Alcian blue dye, Goblet cell marker) (figure 6E). As in the single staining, the Reg1B red staining is prominently found at the crypt base, colocalised with the immunostaining (brown) of lysozyme, and it is adjacent to blue-dyed mucin-positive cells. Although further investigations are needed to understand the nature of these transcriptional changes, our findings indicate that Reg1B is expressed in intestinal villi, especially at the crypt-base, and might be produced and secreted by Paneth cells in response to *A. soehngenii* L2-7 transit. In this regard, the low concentrations of plasma Reg1B, assessed 8 hours postduodenal infusion (at the end of the MMT) (online supplemental figure S5J), suggest that Reg1B is mainly secreted into the (small) intestinal lumen, thereby acting in a paracrine manner on intestinal cells. To understand how *A. soehngenii* L2-7 may regulate Reg1B expression, we further exposed Caco-2 cells for 6 hours to either butyrate or muramyl dipeptide, the bioactive bacterial peptidoglycan motif, and found a marked upregulation of Reg1B by both stimulations (figure 6F,G). In line with this, direct exposure to heat-inactivated *A. soehngenii* L2-7 bacteria upregulates Reg1B expression (online supplemental figure S5L).

Importantly, no carry-over effects were observed between weeks 0 and 4, independently of the intervention order, as shown in online supplemental figure S6 for baseline faecal levels of *A. soehngenii*, faecal butyrate, plasma GLP1 excursions and glucose MAD in the first 24 hours postinfusion (online supplemental figure S6A–D).

DISCUSSION

In this pioneer randomised cross-over phase II trial, we demonstrate the early and wide impact of a single duodenal infusion of *A. soehngenii* L2-7 on the duodenal transcriptomic profile, and moreover, we identify the metabolic parameters being influenced (for up to 24 hours) by a single dose of live *A. soehngenii* L2-7 in treatment-naïve subjects with MetS. Indeed, administration of *A. soehngenii* L2-7 (vs placebo) resulted in an altered small intestinal gene expression signature and, most prominently, in the upregulation of *REG1B*. Moreover, *A. soehngenii* L2-7 infusion induced higher postprandial plasma bile salt and GLP-1 levels as well as lower glucose variability (MAD) within 24 hours after infusion of *A. soehngenii* L2-7. Although further investigations are warranted, these data, combined with our previous studies,[13 14] suggest that *A. soehngenii* L2-7 improves human glucose metabolism in human MetS, likely by shaping BA metabolism and augmenting intestinal GLP-1 production.

We previously showed that, in subjects with metabolic syndrome, oral intake of A. soehngenii L2-7 for 4 weeks increased plasma primary and, particularly, secondary bile acids,[14] which are known to be formed by commensal microbes, such as those belonging to the Ruminococcaceae and Lachnospiraceae.[32 33] Moreover, in db/db mice, 4 week oral *A. soehngenii* treatment alleviated insulin resistance and modified bile salt metabolism in conjunction with augmenting the expression of genes involved in BA metabolism/transport in SI, including suppression of duodenal *Fxr* and *Ost-alpha* expression.[13] Remarkably, we here disclose that a single duodenal infusion of *A. soehngenii*is sufficient to increase secondary BA, of which TDCA, TLCA, GDCA, and isoUDCA associate with increase GLP-1 levels. These findings are in line with previous studies showing that conjugated BA, including TDCA, TLCA, GDCA and UDCA, promote GLP-1 release by intestinal L cells.[34–38] Notably, the genome of *A. soehngenii* harbours a sodium symporter gene (EHLA_2286) as well as two bile salt hydrolase (BSH)-encoding genes (locus tags EHLA_1602 and EHLA_2245).[20] Besides, transcriptome analysis of a simplified microbiota community (harbouring the *A.*

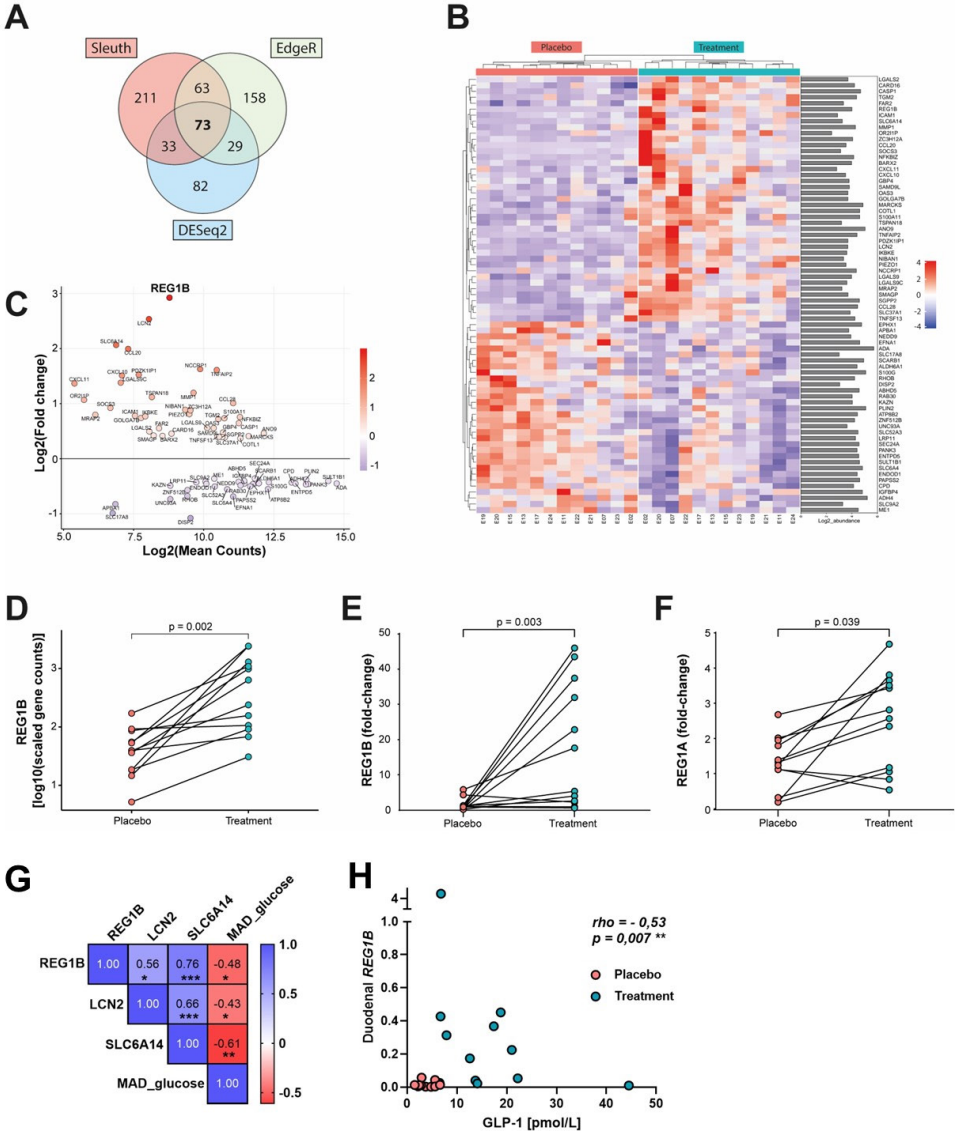

Figure 5 RNAseq (duodenal gene expression). (A) RNAseq data sets analysed by three DGE technologies: Sleuth, EdgeR and DESeq2 were identified. Venn diagram showing the numbers of genes significantly upregulated or downregulated in either one of the pipelines. (B) Heatmap of the 73 top DE genes between placebo and treatment, identified by all three DGE technologies. (C) MA (ratio intensity) plot visualising the gene expression ratios (fold changes treatment vs placebo, Y axis) and the mean expression intensity (average RNAseq counts per gene, X axis) of DE genes. (D) RNAseq read counts of *REG1B* gene, duodenal expression. (E) Gene expression measured by qPCR in duodenal biopsies of *REG1B* and (F) *REG1A*, shown as fold change versus placebo by $2^{-\Delta\Delta Ct}$ data analysis. (G) Correlation heatmap showing Spearman's r rank correlation coefficients and statistically significant correlations. *P≤0.05, **P≤0.01, ***P≤0.001 between duodenal gene expression of *REG1B*, *LCN2*, *SLC6A14* and median absolute deviation of continuous glucose measurements (MAD) over the first 24 hours after placebo/treatment intervention. (H) Spearman's correlation between GLP-1 plasma concentrations 6 hours postinfusion and duodenal gene expression of *REG1B* (assessed by quantitative PCR). DE, differentially expressed; DGE, digital gene expression; GLP-1, glucagon-like peptide 1; RNAseq, RNA sequencing.

soehngenii strain) engrafted in murine guts confirmed that both bsh genes are functionally expressed in the intestinal tract.[21] These findings together with our observations of increased secondary BA on *A. soehngenii* feeding (this study,[14]) point to an active role of this strain in the formation of secondary BA, which may act as GLP-1 secretagogues by binding the TGR5 receptor.[23 39 40] In addition, *A. soehngenii* decreased the duodenal expression of the FXR-target *OSTalpha*,[26] consistent with a de-activation of FXR signalling observed in *A. soehngenii*-treated db/db mice.[13] Notably, FXR suppresses GLP-1 secretion by enteroendocrine L cells, whereas its inhibition improves metabolic control.[24 25 41] Thus, the diminished FXR activation may also account for more GLP-1 availability and, according to the study of Ducastel *et al*, more L cells' responsiveness to butyrate/GPR43 signaling.[25] Indeed, we observed a significant effect of *A. soehngenii* infusion on postprandial levels of GLP-1, but not GIP, suggesting that this strain sensitises L cells to secrete more GLP-1, likely in response to its own metabolites, such as butyrate and secondary (hydrophobic) BA. This hypothesis is supported by animal studies showing that gut microbiota has a rapid and pronounced effect on L cell and GLP-1 content, predominantly in the small intestine, where there is direct contact between enteroendocrine cells and mucosal microbiota.[15 42 43] Moreover, *A. soehngenii* is a known producer of the SCFA butyrate,[10] which by binding its receptor GPR43 expressed on L cells stimulates GLP-1 secretion.[22] Overall, the *A. soehngenii*-mediated increase in plasma

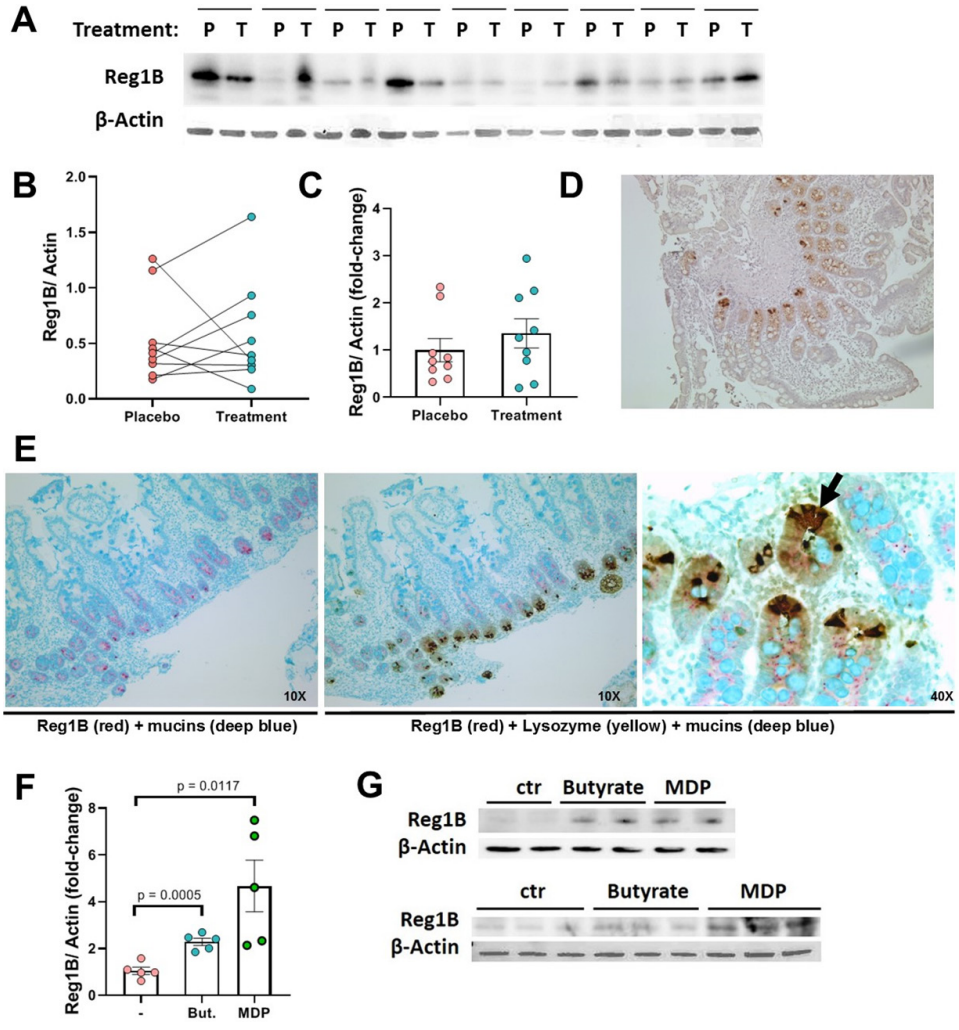

Figure 6 Reg1B expression in duodenum. (A) Western blot image of duodenal lysates blotted with antibodies against Reg1B and β-actin. (B) Quantification of Reg1B expression level in duodenal biopsies, Reg1B expression normalised to β-actin (loading control). (C) Reg1B protein expression shown as fold change treatment versus placebo. (D) Immunohistochemical staining of Reg1B in duodenal biopsies. (E) Sequential immunostaining of duodenal biopsies for Reg1B (red), lysozyme (yellow, Paneth cells) and mucins (deep blue, Goblet cells). Images shown at ×10 or ×40 magnification, as indicated. Arrow indicates one of the Reg1B+lysozyme colocalisation point. (F) Quantification of Reg1B expression level in Caco-2 cells, Reg1B expression normalised to β-actin (loading control); Reg1B expression shown as fold-change treatment versus placebo, but: butyrate 1 mM; MDP: 1 µg/mL. (G) Western blot images of Caco-2 cell lysates blotted with antibodies against Reg1B and β-actin. MDP, muramyl dipeptide.

GLP-1, whether through butyrate/BA signalling and/or FXR inhibition, may justify the observed reduction in glucose MAD after bacteria intake. This improvement in glycaemic variability may be the result of the insulin sensitising effects of butyrate as well as GLP-1.[11 16 17] In addition, we cannot exclude that *A. soehngenii* ameliorates the glycaemic control through alternative (less obvious) mechanisms: for example, by contributing to the generation of microbiota-derived neurotransmitters, in forms of proteins/peptides or gases, which can act locally on gut muscle relaxation or enteric neuron activation as well as distally on the brain influencing appetite, behavior and peripheral glucose homeostasis.[44] Furthermore, a recent study disclosed that the beneficial action of *Akkermansia muciniphila* on the systemic metabolic profile are accounted by a bacterial protein, named P9, of the peptidase S41A family that stimulates, in vivo, thermogenesis and GLP-1 secretion.[45] Curiously, *A. soehngenii* has the genetic capacity to express the peptidase S41 family, underscoring that multiple processes may dictate the observed metabolic benefits of *A. soehngenii*, beyond BA/butyrate production (eg, via production of bioactive molecules or possibly via Reg1B induction).

Although the fold-change comparison of faecal butyrate rates showed that butyrate tended to be higher after *A. soehngenii*-treatment, herewith, we also found a negative effect of placebo infusion on butyrate and acetate concentrations; an effect most likely due to side-effects of glycerol on SCFA production, as earlier described.[46] Nonetheless, SCFA levels remained stable after *A. soehngenii* L2-7 administration suggesting that an increased SCFA production by *A. soehngenii* L2-7 counterbalances the reduction in SCFA caused by glycerol infusion and can hence better modulate intestinal GLP-1 production. In contrast to the changes seen in faecal butyrate, the plasma levels of butyrate were largely unaffected 8 hours after *A. soehngenii*-treatment. This might be due to the fact that microbially-produced butyrate is the primary energy source for colonocytes and hepatic lipid and glucose production[1] rendering more difficult to detect disparities in its circulating peripheral plasma levels. Notwithstanding, we cannot exclude that variations in circulating SCFA

concentrations become evident at a later time-point (eg, 24 hours, as for the faecal SCFA levels).

Being at the interface with intestinal microbiota, duodenal mucosa cells underwent a robust transcriptional reprogramming upon encountering *A. soehngenii* L2-7. The most differentially expressed genes after bacteria administration encode for proteins involved in metabolite transport, cholesterol metabolism or cytokine signalling. Nevertheless, the three most upregulated genes *REG1B*, *LCN2* and *SLC6A14* were found to negatively correlate with glucose MAD rates, hinting to a protective function in glycaemic control. In line, rodent studies demonstrate that increased LCN2 expression promotes glucose tolerance, insulin sensitivity and controls appetite[47], whereas LCN2 deficiency worsens insulin resistance.[48] Similarly, SLC6A14 deficiency in high-fat diet-fed mice worsens adiposity and MetS. Accordingly, the obesity-linked single-nucleotide polymorphism (SNP) in SLC6A14 has been shown to reduce SLC6A14 expression.[49]

The most prominent changes were seen in the expression of *REG1B*, which, along with *REG1A,* was markedly upregulated after *A. soehngenii* L2-7 administration. They are both members of the REG gene family, which was first discovered in pancreas, being expressed mainly by exocrine acinar cells and, upon cellular damage, in the islets of Langerhans.[50] Animal studies using Reg knock-out, overexpression or administration of recombinant REG proteins showed that Reg proteins elicit mitogenic effects on β-cells and protection against diabetes.[28 51 52] However, genomic SNPs in the REG1B were not associated with T2D[53] suggesting that tissue specific expression is more relevant. Similarly to the pancreas, intestinal Reg protein expression has been linked to proliferation being enhanced in inflamed and neoplastic conditions.[54–56] By immunostaining, we found that Reg1B and Reg1A are localised at the base of small-intestinal crypts with Reg1B being more prominently expressed by Paneth cells as compared with its expression (at a lower extent) in enterocytes; this is corroborated by a previous study describing *REG1A*, *REG1B*, and *REG3* gene expression in Paneth cells.[56] Notably, Paneth cells guard $Lgr5^+$ stem cells in the crypt bases through production of signalling and bactericidal molecules. Indeed, Paneth cells have been reported to directly sense indigenous microbes via Toll-like receptor engagement and, thus, limit mucosa penetration by commensals by secreting antimicrobial products, which include Reg3β and Reg3γ proteins.[57] In line with this, we disclose here that in enterocytes, Reg1B expression is triggered by peptidoglycan and butyrate. Although further investigations are needed, we can argue that intestinal epithelial and Paneth cells sense the administered bacteria via GPR and innate immune receptors, resulting in the induction of *REG1* expression. The regenerating activities of Reg proteins on pancreatic cells seem to act in an auto/paracrine manner[50 52]; hence, it is likely that the duodenally secreted Reg1A/B acts locally, possibly inducing progenitor or L-cell hyperplasia. In support of a 'local' effect of Reg1B on intestinal L cells, duodenal *REG1B* levels were significantly associated with GLP-1 concentrations, and Reg1B concentrations were markedly lower in plasma samples than in duodenal tissues. Indeed, Reg1B was non-detectable in plasma samples of six patients 8 hours after placebo intake and in two samples following *A. soehngenii* L2-7 infusion. At protein levels, we did not find statistically significant differences in Reg1B or Reg1A expression in duodenum between placebo and treatment interventions. We therefore feel that this is likely due to their secretion into the intestinal lumen and hence loss of Reg proteins within the duodenal mucosa.[58]

As expected and importantly for the cross-over nature of our study design, the single duodenal bacteria infusion did not affect faecal microbiota composition and Shannon microbial diversity in a major manner, therefore excluding treatment-induced carry-over effects. Accordingly, the order of interventions did not impact the levels of faecal butyrate, postprandial GLP-1 responses nor the 24-hour glucose variability. Also, the lack of fluctuations in faecal *A. soehngenii* L2-7 abundancy over time was anticipated as it is unlikely that a single-dose of 10^{11} bacteria results in colonic colonisation. Notwithstanding, these findings implicate that the herein reported effects of *A. soehngenii* are triggered solely by its transit throughout the gut, and they would be greatly enhanced with a full bacteria engraftment of the SI/colon.

Limitations

Some limitations of this study need to be acknowledged. We administered the bacterial strain only once, as performed by van Baarlen *et al*[59] with a *Lactobacillus* strain; nonetheless, multiple infusions could permit bacteria colonisation of the gut and, consequently, elicit more prominent and lasting metabolic responses. Herein, by using a nosoduodenal infusion, we limited the deleterious effects of stomach acid and oxygen exposure on the viability of *A. soehngenii* L2-7, thus optimising the clinical potential of *A. soehngenii*. Nevertheless, future studies will have to demonstrate whether multiple bacterial administrations *via* duodenal-tube infusions or enteric-coated capsules will result in more pronounced effects.[60]

CONCLUSIONS

To our knowledge, this is the first study to administer a single strain of a strict anaerobe directly into the duodenum to maximally preserve viability bypassing the stomach. Single duodenal infusion of *A. soehngenii* L2-7 resulted in a significantly altered expression of small intestinal genes with the most prominent effect on *REG1B*, which was found to be associated with increased GLP-1 levels and improved peripheral glycaemic control and to be strongly expressed at the base of the intestinal crypts within Paneth cells. Moreover, the infusion of *A. soehngenii* L2-7 rapidly triggers favourable changes in metabolic parameters: it significantly enhances postprandial GLP-1 response (6 hours after intake) and ameliorates blood glucose variability (MAD, first 24 hours). Although *A. soehngenii*-derived bioactive metabolites and the incretin system may drive the improvement in glycaemic control and the insulin-sensitising effects of this strain, further studies are warranted to elucidate the mechanisms underlying the beneficial effects of *A. soehngenii*.

MATERIALS AND METHODS

Patient recruitment and involvement

Twelve Caucasian male subjects (age 21–69 years) with a body mass index between 30 and 43 kg/m^2 were recruited by local newspaper advertisements (period of recruitment and follow-up: December 2017–February 2019). In order to be included in the trial, all subjects had to be treatment-naïve and suffer from MetS, determined by the presence of ≥3 criteria out of the five following criteria: fasting plasma glucose ≥5.6 mmol/L, triglycerides ≥1.7 mmol/L, waist circumference ≥102 cm, high-density lipoprotein cholesterol ≤1.04 mmol/L and blood pressure ≥130/85 mm Hg.[61] Also, HOMA-IR (>2.5) was included as an extra screening marker of insulin resistance. Exclusion criteria included a history of cardiovascular event, cholecystectomy, overt untreated gastrointestinal disease or abnormal bowel habits, liver enzymes>2.5 fold higher than the upper limit of normal range, smoking, alcohol abuse and use of proton pump

inhibitors or antibiotics in the past 3 months. Only men were included in the study to avoid confounding effects on insulin sensitivity due to changes in female hormone concentrations in (postmenopausal) women.[62] Study participants were requested not to alter their physical exercise and dietary patterns after inclusion. The study was registered at the Dutch Trial Register.

Study design

This was a randomised double-blind placebo-controlled cross-over phase II study. All subjects (n=12) received both treatment (10^{11} *A. soehngenii* L2-7 cells, dosage based on our previous study[14]) and placebo (10% glycerol-phosphate-buffered saline, PBS), with a washout period of 4 weeks in between, as depicted in figure 1. The order of administration was randomised in a 1:1 fashion using computerised randomisation and was double-blinded (to patients and doctor in charge). After overnight fasting, a duodenal tube was placed using the electromagnetic-guided system Cortrak. The treatment arm received 10 mL of 10:90 glycerol:PBS solution containing *A. soehngenii* L2-7 (NCBI taxonomy ID 105843)[9] at a concentration of 10^{10} cells/mL (total of 10^{11} cells) infused distally to the papilla of Vater, whereas the placebo arm underwent the same intervention, receiving only 10 mL of vehicle solution (10% glycerol in PBS). Six hours later, a gastroduodenoscopy was performed and duodenal biopsies were taken around the same location as the duodenal infusion and either stored in paraffin for histology or snap-frozen in liquid nitrogen and then stored at −80°C. After the gastroduodenoscopy, a 2-hour MMT was conducted as previously described.[4] Subjects received an intravenous catheter in a distal arm vein over which baseline blood samples were drawn; hereafter, subjects immediately ingested a liquid meal solution (Nutridrink; Nutricia Advanced Medical Nutrition, Amsterdam, Netherlands) containing 600 kcal (35% fat, 49% carbohydrates and 16% proteins) and, for the subsequent 2 hours, blood samples were drawn for postprandial glucose, insulin, triglyceride, GIP and GLP-1 excursions (measured by standard clinical diagnostic methods). Subjects received a continuous glucose monitor (CGM, FreeStyle Libre System, Abbott USA) for 24 hours. Finally, subjects were asked to keep an online nutritional diary to monitor food intake during these days after the intervention (https://mijn.voedingscentrum.nl/nl/eetmeter/) and to collect faecal samples at several time-points (see figure 1). Four weeks after the first visit, the complete study cycle was repeated, switching intervention arms for each patient.

Author affiliations
[1]Vascular Medicine, Amsterdam UMC Locatie AMC, Amsterdam, The Netherlands
[2]Clinical Pharmacy, Amsterdam UMC Locatie AMC, Amsterdam, The Netherlands
[3]Experimental Vascular Medicine, Amsterdam UMC Locatie AMC, Amsterdam, The Netherlands
[4]Microbiology, Wageningen University & Research, Wageningen, The Netherlands
[5]Gastroenterology, Amsterdam UMC Locatie AMC, Amsterdam, The Netherlands
[6]Biomedical Sciences, University of Copenhagen Novo Nordisk Foundation Center for Basic Metabolic Research, Kobenhavn, Denmark
[7]Wallenberg Laboratory for Cardiovascular and Metabolic Research, University of Gothenburg, Goteborg, Sweden
[8]Center for Microbiome and Human Health, Lerner Research Institute, Cleveland Clinic, Cleveland, Ohio, USA
[9]Cardiovascular and Metabolic Sciences, Lerner Research Institute, Cleveland Clinic, Cleveland, Ohio, USA
[10]Human Microbiome Research Program, University of Helsinki, Helsinki, Finland

Acknowledgements We acknowledge Dr S Shetty and Dr H Heilig (Microbiology Lab, Wageningen University, The Netherlands), respectively, for helpful suggestions and DNA isolations from biopsies for *Anaerobutyricum soehngenii* L2-7 detection.

Contributors AK, AKG, ES, WMDV, MN and ER designed the study. AK, KW, JW, SM, HH, MW, SA, SH, HL, EMK, BH, JH, JJGHMB, MS, FB, ER, P-OB, JvS, MB, DMB, CMS and SLH performed the research. AK, ER, AP and EL performed the statistical analysis. AK, WMDV, AKG, MN and ER drafted the paper. All authors critically reviewed and approved the manuscript. ER acts as guarantor for this study and publication.

Funding MN is supported by a ZONMW VICI grant 2020 (number 09150182010020). WMDV is supported by the SIAM Gravitation Grant (024.002.002) and the 2008 Spinoza Award of The Netherlands Organization for Scientific Research. KW, MB, JvS, DMB and ER are appointed on a CAMIT grant 2018 (to MN and FB). The study reported here was additionally supported by Le Ducq consortium grant 17CVD01 to SLH and MN (on which HJH and CMS are appointed). MN and AGK are supported by a Dutch Heart Foundation CVON IN CONTROL-2 consortium grant.

Competing interests MN is in the scientific board of Kaleido Biosciences, Boston USA. WMDV is founder and in the board of A-mansia, Belgium. FB is in the scientific board of Metabogen AB, Sweden. MN and WMDV are founders and Scientific Advisory Board members of Caelus Pharmaceuticals, the Netherlands. SLH is a paid consultant for P&G and coinventor on pending and issued patents held by the Cleveland Clinic, and is eligible for receiving payments for inventions or discoveries related to cardiovascular diagnostics or therapeutics from Cleveland HeartLab, Quest Diagnostics and P&G.

Patient consent for publication Not applicable.

Ethics approval The study was approved by the local institutional review board of the Amsterdam University Medical Center in Amsterdam, the Netherlands, and conducted in accordance with the Declaration of Helsinki. Patients were not involved in the design and conduct of this research, although they were thoroughly informed about the procedures and goals of the study on recruitment visits. All participants signed a written informed consent.

Provenance and peer review Not commissioned; externally peer reviewed.

Data availability statement All data relevant to the study are included in the article or uploaded as supplementary information.

ORCID iDs
Koen Wortelboer http://orcid.org/0000-0002-3582-0127
Andrei Prodan http://orcid.org/0000-0003-2789-7789
Jacques J G H M Bergman http://orcid.org/0000-0001-7548-6955
Jamie van Son http://orcid.org/0000-0002-9876-2876
Diogo Mendes Bastos http://orcid.org/0000-0001-7343-1192
Willem M De Vos http://orcid.org/0000-0002-0273-3166
Max Nieuwdorp http://orcid.org/0000-0002-1926-7659
Elena Rampanelli http://orcid.org/0000-0002-7742-0092

REFERENCES

1 Warmbrunn MV, Herrema H, Aron-Wisnewsky J, *et al*. Gut microbiota: a promising target against cardiometabolic diseases. *Expert Rev Endocrinol Metab* 2020;15:13–27.
2 Ridaura VK, Faith JJ, Rey FE, *et al*. Gut microbiota from twins discordant for obesity modulate metabolism in mice. *Science* 2013;341:1241214.
3 Vrieze A, Van Nood E, Holleman F, *et al*. Transfer of intestinal microbiota from lean donors increases insulin sensitivity in individuals with metabolic syndrome. *Gastroenterology* 2012;143:913–6.
4 Kootte RS, Levin E, Salojärvi J, *et al*. Improvement of insulin sensitivity after lean donor feces in metabolic syndrome is driven by baseline intestinal microbiota composition. *Cell Metab* 2017;26:611–9.
5 Pedersen HK, Gudmundsdottir V, Nielsen HB, *et al*. Human gut microbes impact host serum metabolome and insulin sensitivity. *Nature* 2016;535:376–81.
6 Thingholm LB, Rühlemann MC, Koch M, *et al*. Obese individuals with and without type 2 diabetes show different gut microbial functional capacity and composition. *Cell Host Microbe* 2019;26:e10:252–64.

7 Karlsson FH, Tremaroli V, Nookaew I, *et al*. Gut metagenome in European women with normal, impaired and diabetic glucose control. *Nature* 2013;498:99–103.
8 Le Chatelier E, Nielsen T, Qin J, *et al*. Richness of human gut microbiome correlates with metabolic markers. *Nature* 2013;500:541–6.
9 Shetty SA, Zuffa S, Bui TPN, *et al*. Reclassification of eubacterium hallii as anaerobutyricum hallii gen. nov., comb. nov., and description of anaerobutyricum soehngenii sp. nov., a butyrate and propionate-producing bacterium from infant faeces. *Int J Syst Evol Microbiol* 2018;68:3741–6.
10 Duncan SH, Louis P, Flint HJ. Lactate-utilizing bacteria, isolated from human feces, that produce butyrate as a major fermentation product. *Appl Environ Microbiol* 2004;70:5810–7.
11 Gao Z, Yin J, Zhang J, *et al*. Butyrate improves insulin sensitivity and increases energy expenditure in mice. *Diabetes* 2009;58:1509–17.
12 Bouter K, Bakker GJ, Levin E, *et al*. Differential metabolic effects of oral butyrate treatment in lean versus metabolic syndrome subjects. *Clin Transl Gastroenterol* 2018;9:155.
13 Udayappan S, Manneras-Holm L, Chaplin-Scott A, *et al*. Oral treatment with *Eubacterium hallii* improves insulin sensitivity in *db/db* mice. *NPJ Biofilms Microbiomes* 2016;2:16009.
14 Gilijamse PW, Hartstra AV, Levin E, *et al*. Treatment with Anaerobutyricum soehngenii: a pilot study of safety and dose–response effects on glucose metabolism in human subjects with metabolic syndrome. *NPJ Biofilms Microbiomes* 2020;6:1–10.
15 Greiner TU, Bäckhed F. Microbial regulation of GLP-1 and L-cell biology. *Mol Metab* 2016;5:753–8.
16 Jiang Y, Wang Z, Ma B, *et al*. Glp-1 improves adipocyte insulin sensitivity following induction of endoplasmic reticulum stress. *Front Pharmacol* 2018;9:1–10.
17 Guo C, Huang T, Chen A, *et al*. Glucagon-like peptide 1 improves insulin resistance in vitro through anti-inflammation of macrophages. *Braz J Med Biol Res* 2016;49:1–9.
18 Louis P, Young P, Holtrop G, *et al*. Diversity of human colonic butyrate-producing bacteria revealed by analysis of the butyryl-CoA:acetate CoA-transferase gene. *Environ Microbiol* 2010;12:304–14.
19 Engels C, Ruscheweyh H-J, Beerenwinkel N, *et al*. The common gut microbe eubacterium hallii also contributes to intestinal propionate formation. *Front Microbiol* 2016;7:1–12.
20 Shetty SA, Ritari J, Paulin L, *et al*. Complete genome sequence of *Eubacterium hallii* strain L2-7. *Genome Announc* 2017;5:4–5.
21 Kovatcheva-Datchary P, Shoaie S, Lee S, *et al*. Simplified intestinal microbiota to study microbe-diet-host interactions in a mouse model. *Cell Rep* 2019;26:3772–83.
22 Tolhurst G, Heffron H, Lam YS, *et al*. Short-chain fatty acids stimulate glucagon-like peptide-1 secretion via the G-protein-coupled receptor FFAR2. *Diabetes* 2012;61:364–71.
23 Thomas C, Gioiello A, Noriega L, *et al*. Tgr5-mediated bile acid sensing controls glucose homeostasis. *Cell Metab* 2009;10:167–77.
24 Trabelsi M-S, Daoudi M, Prawitt J, *et al*. Farnesoid X receptor inhibits glucagon-like peptide-1 production by enteroendocrine L cells. *Nat Commun* 2015;6:1–13.
25 Ducastel S*et al*. The nuclear receptor FXR inhibits glucagon-like peptide-1 secretion in response to microbiota-derived short-chain fatty acids. *Sci. Rep* 2020;10:1–10.
26 Landrier JF, Eloranta JJ, Vavricka SR, *et al*. The nuclear receptor for bile acids, FXR, transactivates human organic solute transporter-α and -β genes. *Am. J. Physiol. - Gastrointest. Liver Physiol* 2006;290:476–85.
27 Inagaki T, Choi M, Moschetta A, *et al*. Fibroblast growth factor 15 functions as an enterohepatic signal to regulate bile acid homeostasis. *Cell Metab* 2005;2:217–25.
28 Unno M*et al*. Production and characterization of reg knockout mice: reduced proliferation of pancreatic β-cells in reg knockout mice. *Diabetes* 2002;51.
29 Gross DJ, Weiss L, Reibstein I, *et al*. Amelioration of diabetes in nonobese diabetic mice with advanced disease by linomide-induced immunoregulation combined with reg protein treatment. *Endocrinology* 1998;139:2369–74.
30 Cui W, De Jesus K, Zhao H, *et al*. Overexpression of Reg3alpha increases cell growth and the levels of cyclin D1 and CDK4 in insulinoma cells. *Growth Factors* 2009;27:195–202.
31 Zheng, H. et al. expression profile of the reg gene family in colorectal carcinoma. *J Histochem Cytochem* 2011;59:106–15.
32 Begley M, Hill C, Gahan CGM. Bile salt hydrolase activity in probiotics. *Appl Environ Microbiol* 2006;72:1729–38.
33 Id MHF, Id SOF, Id RB, *et al*. Bile salt hydrolases : Gatekeepers of bile acid metabolism and host-microbiome crosstalk in the gastrointestinal tract. *PLOS Pathog* 2019:1–6.
34 Brighton CA*et al*. Bile acids trigger GLP-1 release predominantly by accessing Basolaterally located G protein-coupled bile acid receptors. *Endocrinology* 2015;156:3961–70.
35 Kuhre RE, Wewer Albrechtsen NJ, Larsen O, *et al*. Bile acids are important direct and indirect regulators of the secretion of appetite- and metabolism-regulating hormones from the gut and pancreas. *Mol Metab* 2018;11:84–95.
36 van Nierop FS, Meessen ECE, Nelissen KGM, *et al*. Differential effects of a 40-hour fast and bile acid supplementation on human GLP-1 and FGF19 responses. *Am J Physiol Endocrinol Metab* 2019;317:E494–502.
37 Calderon G, McRae A, Rievaj J, *et al*. Ileo-colonic delivery of conjugated bile acids improves glucose homeostasis via colonic GLP-1-producing enteroendocrine cells in human obesity and diabetes. *EBioMedicine* 2020;55:102759.
38 Murakami M, Une N, Nishizawa M, *et al*. Incretin secretion stimulated by ursodeoxycholic acid in healthy subjects. *Springerplus* 2013;2:20.
39 Katsuma S, Hirasawa A, Tsujimoto G. Bile acids promote glucagon-like peptide-1 secretion through TGR5 in a murine enteroendocrine cell line STC-1. *Biochem Biophys Res Commun* 2005;329:386–90.
40 Brighton CA, Rievaj J, Kuhre RE, *et al*. Bile acids trigger GLP-1 release predominantly by accessing basolaterally located G protein-coupled bile acid receptors. *Endocrinology* 2015;156:3961–70.
41 Jiang C, Xie C, Lv Y, *et al*. Intestine-selective farnesoid X receptor inhibition improves obesity-related metabolic dysfunction. *Nat Commun* 2015;6:10166.
42 Arora T, Akrami R, Pais R, *et al*. Microbial regulation of the L cell transcriptome. *Sci Rep* 2018;8:1–9.
43 Cani PD, Hoste S, Guiot Y, *et al*. Dietary non-digestible carbohydrates promote L-cell differentiation in the proximal colon of rats. *Br J Nutr* 2007;98:32–7.
44 Knauf C, Abot A, Wemelle E, *et al*. Targeting the Enteric Nervous System to Treat Metabolic Disorders? "Enterosynes" as Therapeutic Gut Factors. *Neuroendocrinology* 2020;110:139–46.
45 Yoon HS, Cho CH, Yun MS, *et al*. Akkermansia muciniphila secretes a glucagon-like peptide-1-inducing protein that improves glucose homeostasis and ameliorates metabolic disease in mice. *Nat Microbiol* 2021;6:563–73.
46 De Weirdt R, Possemiers S, Vermeulen G, *et al*. Human faecal microbiota display variable patterns of glycerol metabolism. *FEMS Microbiol Ecol* 2010;74:601–11.
47 Mosialou I, Shikhel S, Liu J-M, *et al*. MC4R-dependent suppression of appetite by bone-derived lipocalin 2. *Nature* 2017;543:385–90.
48 Guo H, Jin D, Zhang Y, *et al*. Lipocalin-2 deficiency impairs thermogenesis and potentiates diet-induced insulin resistance in mice. *Diabetes* 2010;59:1376–85.
49 Sivaprakasam S, Sikder MOF, Ramalingam L, *et al*. Slc6A14 deficiency is linked to obesity, fatty liver, and metabolic syndrome but only under conditions of a high-fat diet. *Biochim Biophys Acta Mol Basis Dis* 2021;1867:166087.
50 Baeza N, Sanchez D, Christa L, *et al*. Pancreatitis-associated protein (HIP/PAP) gene expression is upregulated in NOD mice pancreas and localized in exocrine tissue during diabetes. *Digestion* 2001;64:233–9.
51 Takasawa S, Ikeda T, Akiyama T, *et al*. Cyclin D1 activation through ATF-2 in Reg-induced pancreatic beta-cell regeneration. *FEBS Lett* 2006;580:585–91.
52 Xiong X, Wang X, Li B, *et al*. Pancreatic islet-specific overexpression of Reg3β protein induced the expression of pro-islet genes and protected the mice against streptozotocin-induced diabetes mellitus. *Am J Physiol Endocrinol Metab* 2011;300:E669–80.
53 Banchuin N, Boonyasrisawat W, Pulsawat P, *et al*. No abnormalities of Reg1 alpha and Reg1 beta gene associated with diabetes mellitus. *Diabetes Res Clin Pract* 2002;55:105–11.
54 Tsuchida C, Sakuramoto-Tsuchida S, Taked M, *et al*. Expression of *REG* family genes in human inflammatory bowel diseases and its regulation. *Biochem Biophys Rep* 2017;12:198–205.
55 Zheng H-chuan, Sugawara A, Okamoto H, Zheng HC, *et al*. Expression profile of the reg gene family in colorectal carcinoma. *J Histochem Cytochem* 2011;59:106–15.
56 van Beelen Granlund A, Østvik AE, Brenna Øystein, *et al*. Reg gene expression in inflamed and healthy colon mucosa explored by in situ hybridisation. *Cell Tissue Res* 2013;352:639–46.
57 Vaishnava S, Behrendt CL, Ismail AS, *et al*. Paneth cells directly sense gut commensals and maintain homeostasis at the intestinal host-microbial interface. *Proc Natl Acad Sci U S A* 2008;105:20858–63.
58 Peterson KM, Buss J, Easley R, *et al*. REG1B as a predictor of childhood stunting in Bangladesh and Peru. *Am J Clin Nutr* 2013;97:1129–33.
59 van Baarlen P, Troost FJ, van Hemert S, *et al*. Differential NF-kappaB pathways induction by Lactobacillus plantarum in the duodenum of healthy humans correlating with immune tolerance. *Proc Natl Acad Sci U S A* 2009;106:2371–6.
60 Del Piano M, Carmagnola S, Andorno S, *et al*. Evaluation of the intestinal colonization by microencapsulated probiotic bacteria in comparison with the same uncoated strains. *J Clin Gastroenterol* 2010;44 Suppl 1:42–6.
61 Alberti KGMM, Zimmet P, Shaw J. Metabolic syndrome--a new world-wide definition. a consensus statement from the International diabetes federation. *Diabet Med* 2006;23:469–80.
62 Brown MD*et al*. Insulin sensitivity in postmenopausal women. *Diabetes Care* 2000;23:1731–6.

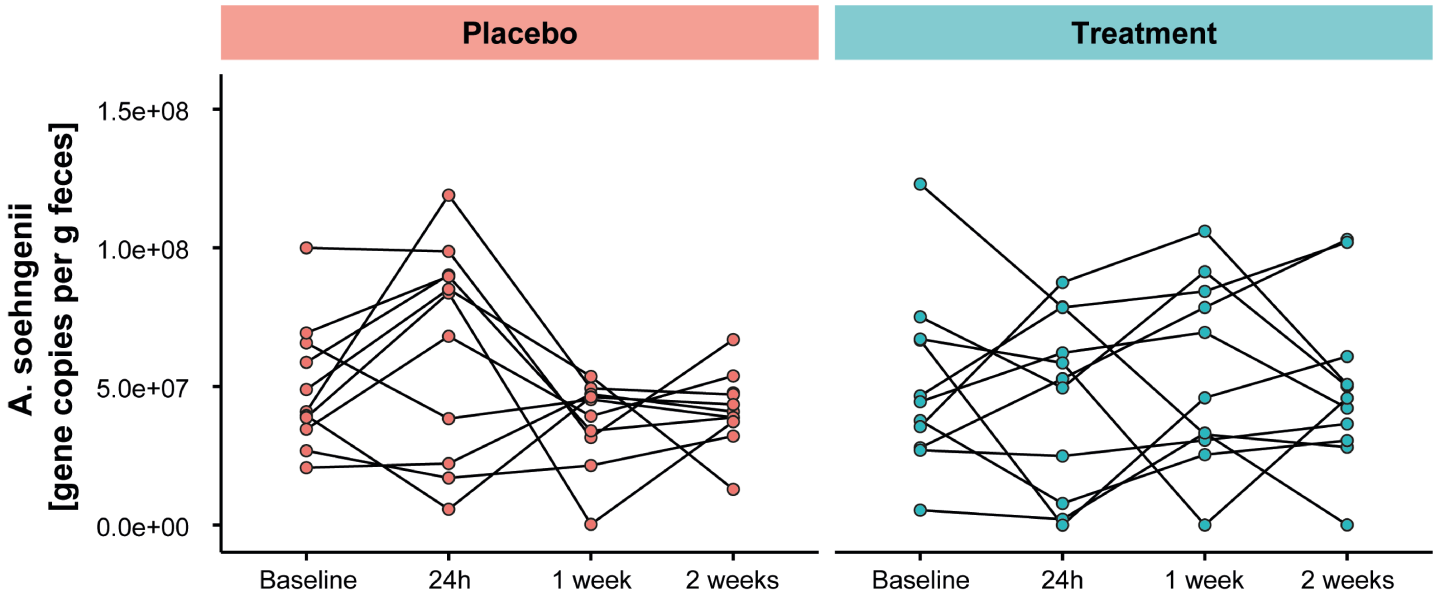
Placebo
Treatment
A. soehngenii
[gene copies per g feces]
1.5e+08
1.0e+08
5.0e+07
0.0e+00
Baseline
24h
1 week
2 weeks
Baseline
24h
1 week
2 weeks

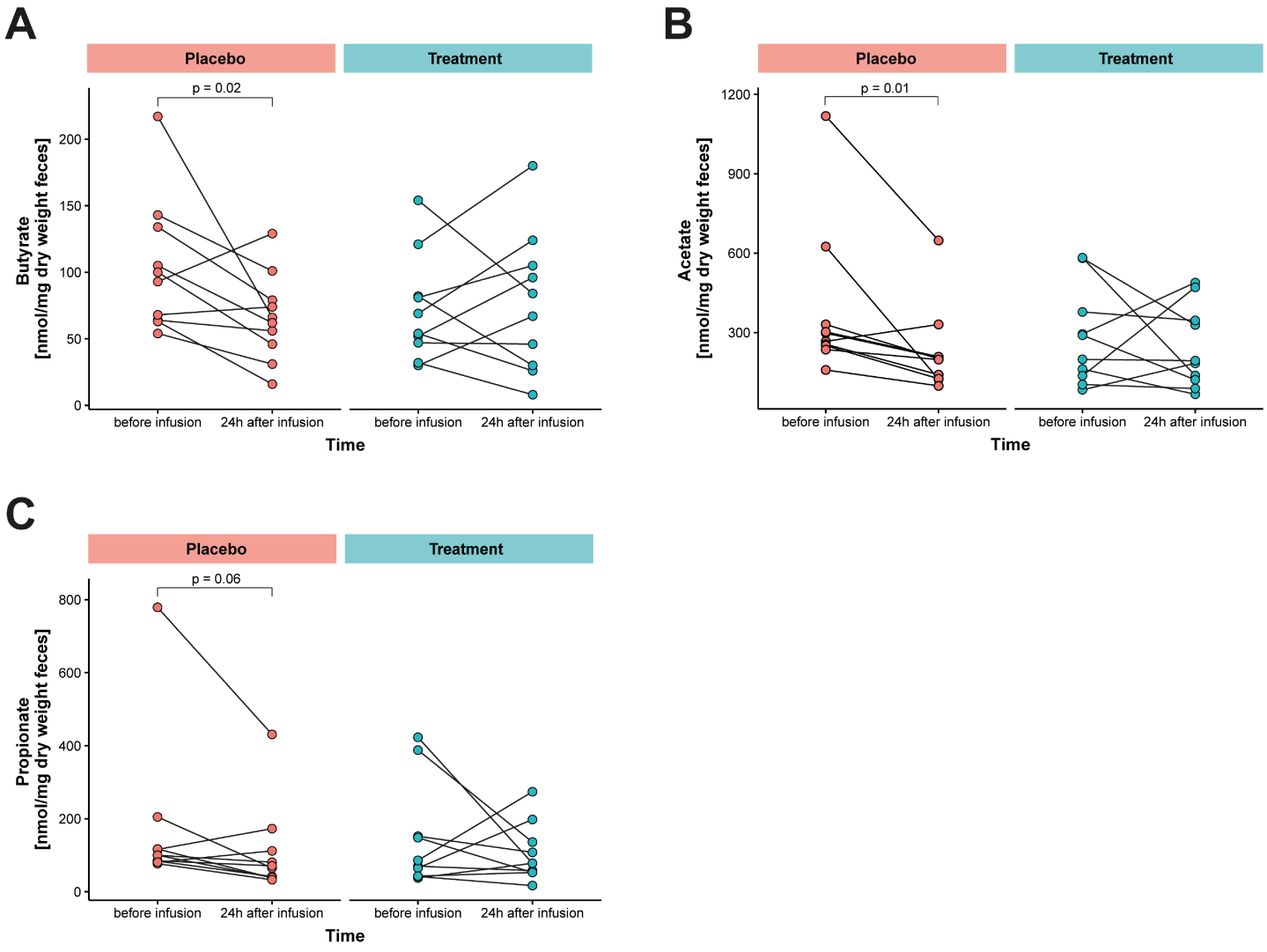
A
Placebo
Treatment
p = 0.02
Butyrate [nmol/mg dry weight feces]
0
50
100
150
200
before infusion
24h after infusion
Time
B
Placebo
Treatment
p = 0.01
Acetate [nmol/mg dry weight feces]
300
600
900
1200
before infusion
24h after infusion
Time
C
Placebo
Treatment
p = 0.06
Propionate [nmol/mg dry weight feces]
0
200
400
600
800
before infusion
24h after infusion
Time

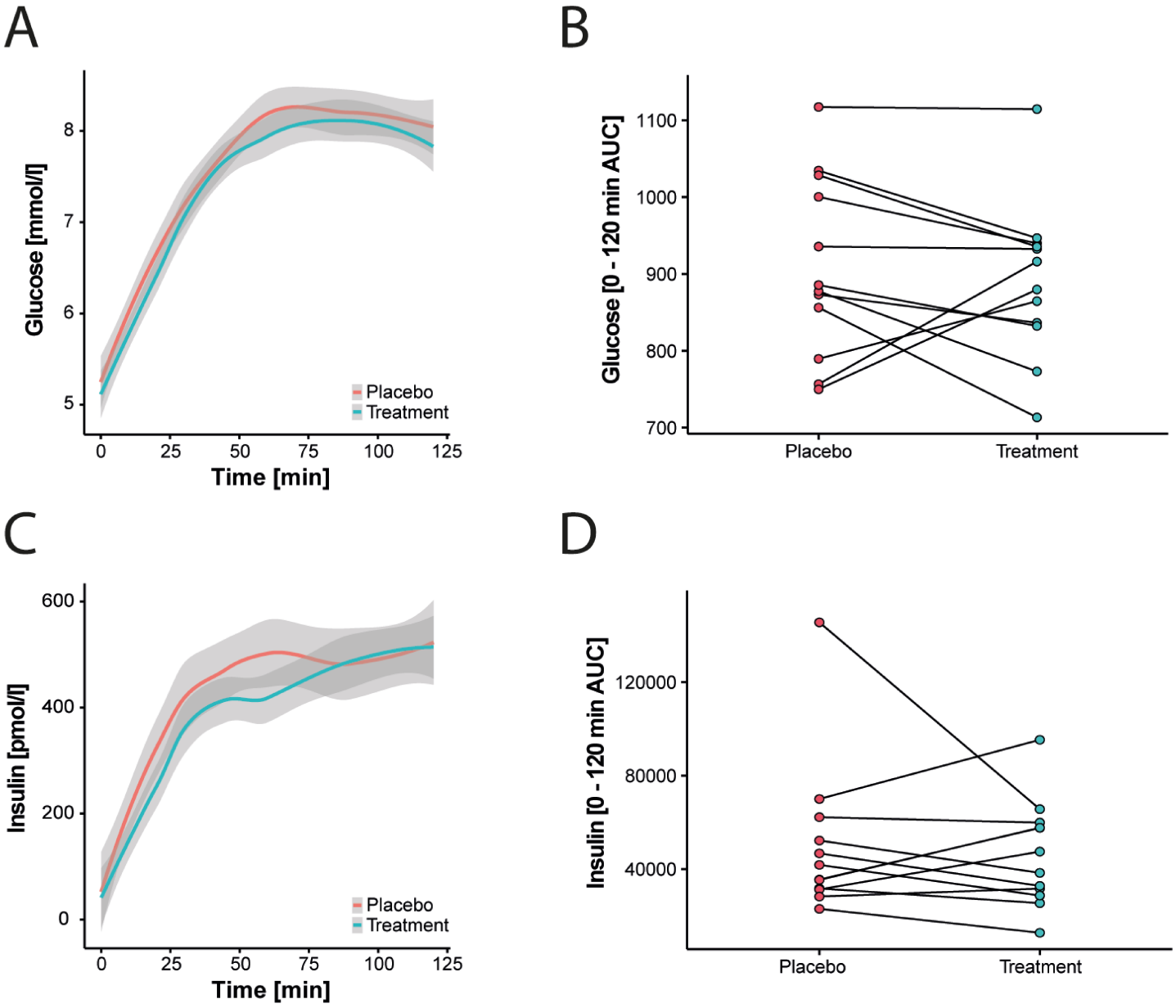
A
Glucose [mmol/l]
8
7
6
5
0
25
50
75
100
125
Time [min]
Placebo
Treatment
B
Glucose [0 - 120 min AUC]
1100
1000
900
800
700
Placebo
Treatment
C
Insulin [pmol/l]
600
400
200
0
0
25
50
75
100
125
Time [min]
Placebo
Treatment
D
Insulin [0 - 120 min AUC]
120000
80000
40000
Placebo
Treatment

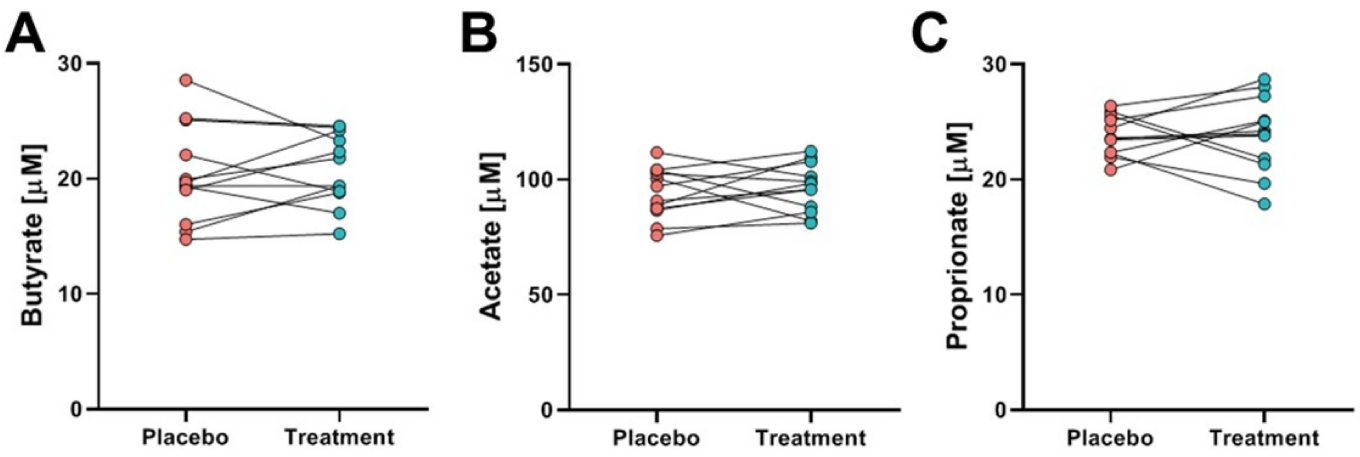
A
Butyrate [µM]
30
20
10
0
Placebo
Treatment
B
Acetate [µM]
150
100
50
0
Placebo
Treatment
C
Proprionate [µM]
30
20
10
0
Placebo
Treatment

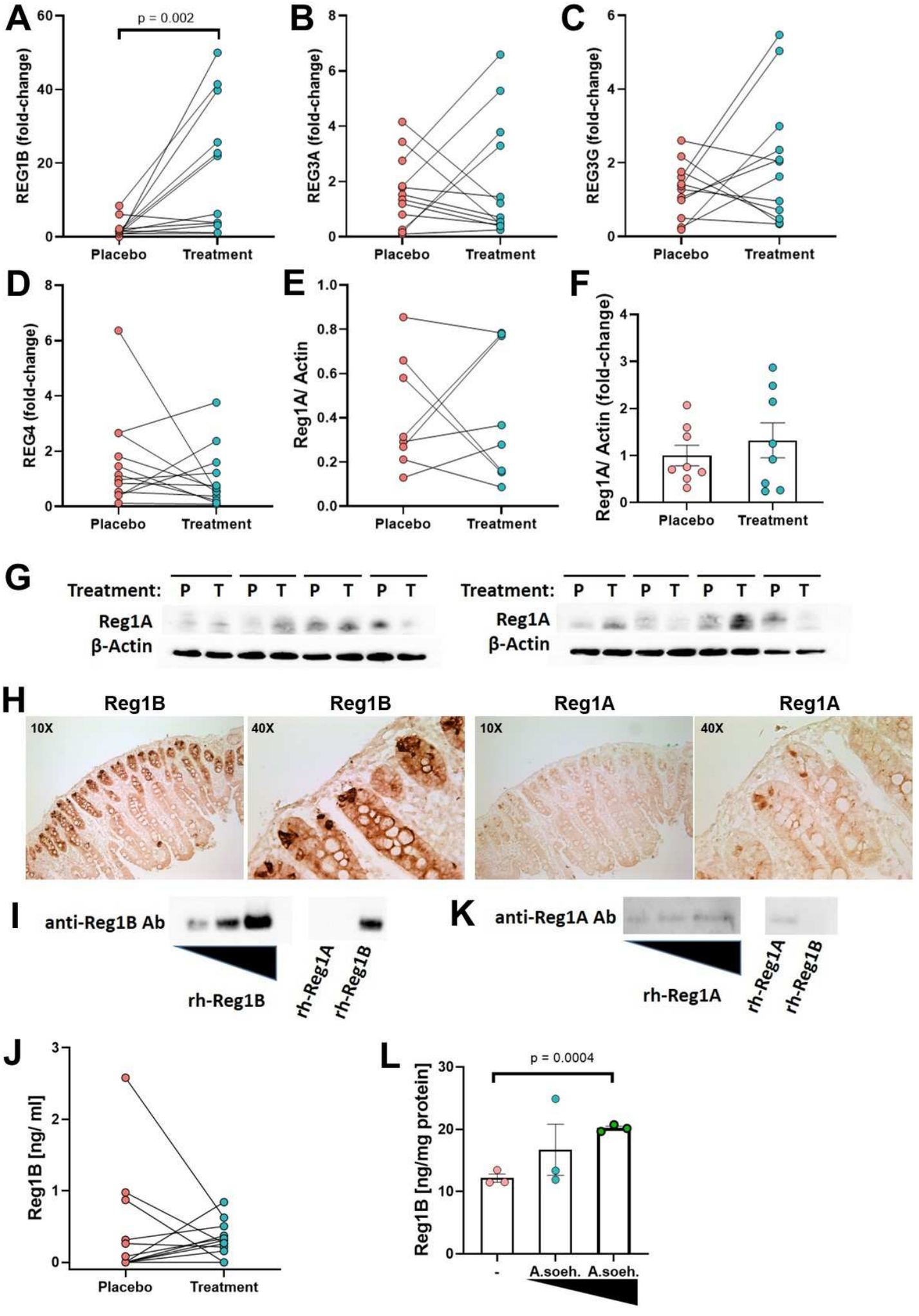
A
p = 0.002
REG1B (fold-change)
Placebo
Treatment
B
REG3A (fold-change)
C
REG3G (fold-change)
D
REG4 (fold-change)
E
Reg1A/ Actin
F
Reg1A/ Actin (fold-change)
G
Treatment: P T P T P T P T
Reg1A
β-Actin
H
Reg1B
Reg1A
10X
40X
I
anti-Reg1B Ab
rh-Reg1B
rh-Reg1A
rh-Reg1B
K
anti-Reg1A Ab
rh-Reg1A
J
Reg1B [ng/ ml]
L
p = 0.0004
Reg1B [ng/mg protein]
-
A.soeh.
A.soeh.

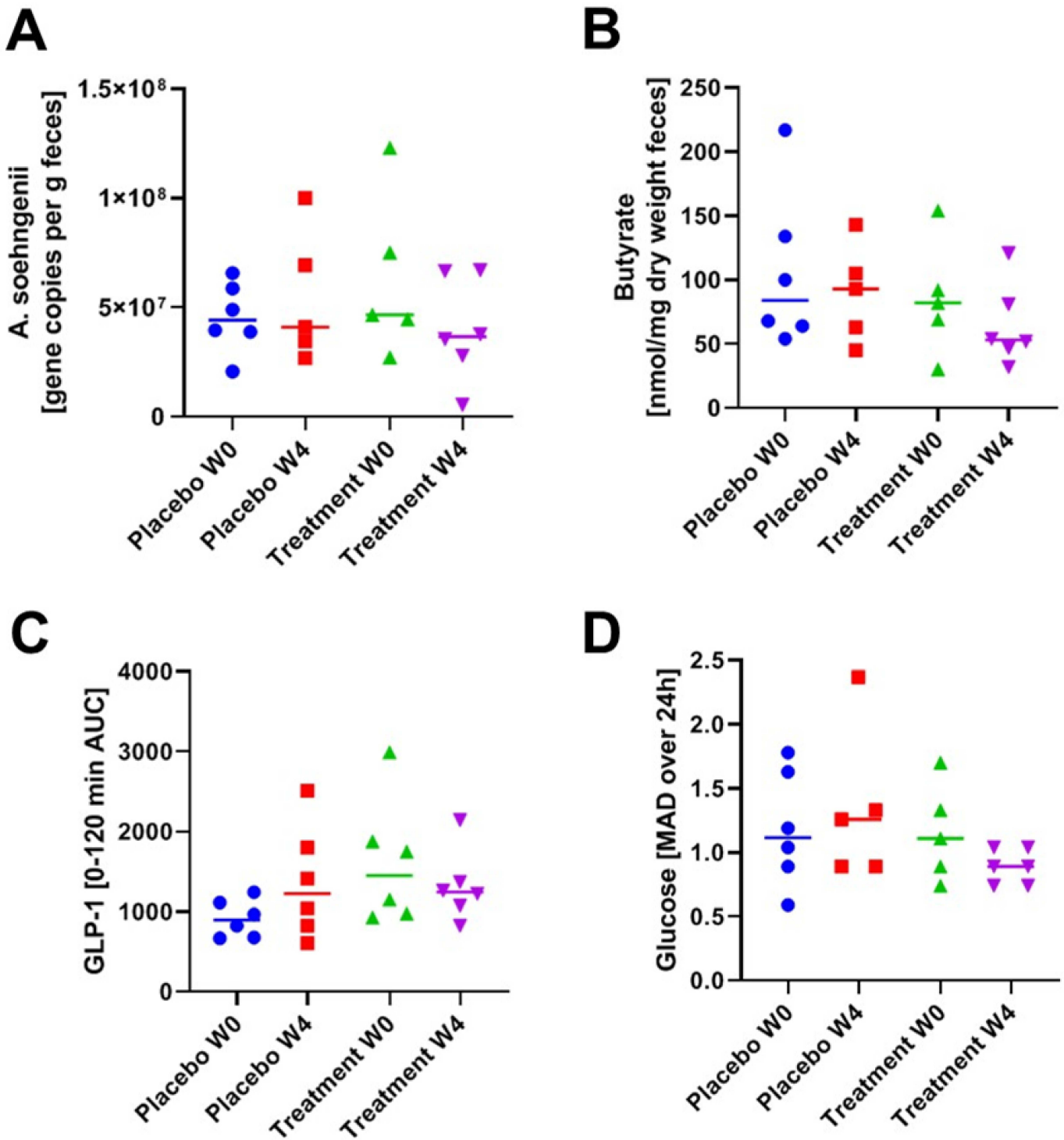
A
A. soehngenii [gene copies per g feces]
1.5×10⁸
1×10⁸
5×10⁷
0
Placebo W0
Placebo W4
Treatment W0
Treatment W4
B
Butyrate [nmol/mg dry weight feces]
250
200
150
100
50
0
Placebo W0
Placebo W4
Treatment W0
Treatment W4
C
GLP-1 [0-120 min AUC]
4000
3000
2000
1000
0
Placebo W0
Placebo W4
Treatment W0
Treatment W4
D
Glucose [MAD over 24h]
2.5
2.0
1.5
1.0
0.5
0.0
Placebo W0
Placebo W4
Treatment W0
Treatment W4

Supplementary Material (Supplementary Material and Methods and Supplementary Figures) for:

Duodenal *Anaerobutyricum soehngenii* infusion stimulates GLP-1 production, ameliorates glycemic control and beneficially shapes the duodenal transcriptome in metabolic syndrome subjects; a randomized double-blind placebo-controlled cross-over study.

Supplementary Material and Methods

Culturing of *A. soehngenii*

The cells were obtained as described previously[1] by culturing *A. soehngenii L2-7* at 500-liter scale in a basic phosphate-bicarbonate salt medium containing 2% yeast extract, 0.4% soy peptone, and 2% sucrose, at pH 6.8 and 37C. Following autoclaving, filter-sterilized components were added, including cysteine (final concentration 0.05%) and a 1 ml per liter of a vitamin solution (containing per liter 10 mg biotin, 10 mg cobalamin, 30 mg para-aminobenzoic acid, 50 mg folic acid, and 150 mg pyridoxamine). *A. soehngenii* L2-7 cells were harvested by microfiltration, washed with PBS, and finally stored in PBS containing 10% glycerol at a concentration of 10^{10} cells/ml in 10 ml tubes at -80°C. *A. soehngenii* L2-7 was handled under strict anaerobic conditions which were maintained during all stages of the production of the concentrated cells: during growth, microfiltration, glycerol mixing, and filling of the tubes with a nitrogen atmosphere. The viability of *A. soehngenii* L2-7 in randomly selected tubes (stored at -80°C at the AMC Department of Clinical Pharmacy) was tested every 6 months during the study using most probable number (MPN) analysis in YCFA medium. MPN analyses were performed in duplicate in anoxic YCFA medium containing sucrose incubated at 37°C for 5 days[1]. Growth was scored by visual and microscopic inspection. Viability stayed constant at 10^{10} cells/ml during the time of the study.

Duodenal RNA sequencing and differential gene expression analysis

RNA for RNA sequencing analysis was isolated from duodenum biopsies, which were directly snap-frozen in liquid nitrogen after biopsy and stored at -80˚C until analysis, from all 12 included participants, using an RNA isolation protocol optimized for small tissue biopsies. In short, biopsies were mixed with 300 µl TriPure (Roche, Basel, Switzerland) and homogenized on ice using a sterile, RNAse free pestle. After short centrifugation, 60 µl of chloroform was added. Samples were then added to a Heavy Phase Lock gel tube (Quanta Bio, Beverly, USA) and centrifuged (15 min, 12.000 x g, 4˚C). The aqueous phase was transferred and mixed with 1 volume of 70% ethanol. The mixture was added to a RNeasy MinElute spin column (QIAgen, Tegelen, the Netherlands). RNA was washed according to manufacturer's protocol and eluted in 14 µl RNAse free water. RNA concentration was measured using the NanoDrop 1000 (Thermo Scientific, Landsmeer, the Netherlands). RIN scores were assessed on a Bioanalyzer 2100 using Eukaryote Total RNA Nano chips (Agilent Technologies, Santa

Clara, USA). RNA was depleted from rRNA and sequenced on a HiSeq4000 (paired-end, 150 bp) by Genomescan BV, Amsterdam, The Netherlands.

RNA raw sequence quality was checked using FastQC (v0.11.9)[2] and quality trimmed and filtered using Trimmomatic (v0.38)[3]. The single, 50 bp reads were processed by removing the first 5 bases, applying a sliding-window quality trim 4 bp wide with a threshold of Q15, then removing all reads shorter than 36 bp after trimming. Quality checked and trimmed reads were subsequently pseudo aligned to the human transcriptome (GRCh38 release 97) using Kallisto (v0.46.0)[4]. The transcript-level counts from Kallisto output were used to perform differential gene expression analysis using 3 different R packages: sleuth (v0.30.0)[5], DESeq2 (v1.28.1)[6], and edgeR (v3.30.3)[7–10]. Count data was imported to DESeq2 and edgeR using the tximport package[11]. Transcript to gene mappings were obtained using the biomaRt package (v2.44.0)[12]. In all 3 workflows, likelihood ratio tests were applied using '~ Subject + Visit' as the full model design and '~ Subject' as the reduced model in order to detect genes that were differentially expressed after *A. soehngenii L2-7* infusion compared to after placebo infusion. All p-values were adjusted for multiple comparisons using the Benjamini-Hochberg method[13]. Significance thresholds were 0.05 for sleuth and edgeR and 0.10 for DESeq2. Only genes found to be differentially expressed by all 3 workflows were examined in downstream analyses.

Real Time quantitative polymerase chain reaction (RT-qPCR)

Total RNA was extracted from frozen duodenal biopsies from 12 patients as described above. Briefly, 1μg of RNA was converted to cDNA with iScript cDNA synthesis kit (BioRad, Veenendaal, The Netherlands). qPCR was performed on a ViiA7 PCR machine (Applied Biosystems, Bleiswijk, The Netherlands). using Sybr Green Fast (Bioline Meridian Bioscience, Cincinnati, Ohio, USA). Gene expression was normalized towards the housekeeping gene Actin, and relative gene expression was calculated with the "delta delta Ct" method and shown as 2ˆ-delta delta Ct. Primer sequences are outlined in Supplementary Table 2; all primers were manufactured by Sigma-Aldrich (Zwijndrecht, The Netherlands).

Western blotting

Duodenal biopsies (from 8/9 patients) were lysated in RIPA buffer (Thermo Fisher Scientific, Breda, The Netherlands) containing protease and phosphatase inhibitors (cOmplete™ Protease inhibitor and PhosSTOP Phosphatase Inhibitor Cocktails, Sigma, Zwijndrecht, The Netherlands) using a ceramic beads homogenizer. For westernblotting of cell lysates, Caco-2 cells were incubated for 30 minutes 4˚C in RIPA buffer supplemented with protease and phosphatase inhibitors. BCA protein assay kit (Thermo Fisher) was used to determine protein concentrations.β-mercaptoethanol was added as reducing agent to all sample lysates, which were run on 4-12% polyacrylamide gels (BioRad, GE, Boston, USA) in MES running buffer. Proteins were transferred to PVDF membranes (BioRad) and were blocked using 5% milk in TBS-T (Tris Buffered Saline – Tween-20). Membranes were incubated

overnight a 4˚C with primary polyclonal rabbit antibodies anti-Reg1B (for Figure 6A/6G: 1:500, E-AB-52897, Elabscience, Houston, USA) and Actin (AB306371, Abcam, Cambridge, UK) or anti –Reg1A (for Figure S5G: 1:500, orb100720, Biorbyt, Cambridge, UK). Horseradish peroxidase (HRP)-conjugated secondary antibodies (R&D systems, Minneapolis, USA) were incubated for 1hour at room temperature. HRP activity was visualized with peroxidase substrate for enhanced chemiluminescence and imaged with ChemiDoc MP Imaging System (BioRad) using Image Lab software (BioRad). Densitometric quantification analysis was performed using the Image J software. All protein levels were normalized to the loading control (β-actin). Reg1B protein expression shown as ratio of densitometric quantification of Reg1B versus β-actin and as intraindividual fold-changes of treatment versus placebo (expression rates of placebo group normalized to mean to represent distribution in expression levels among subjects). In order to show lack of cross-reactivity of the antibodies anti-Reg1B and anti-Reg1A, recombinant Reg1A (Prospec) and Reg1B (Sino Biological) proteins were loaded on polyacrylamide gels and immunoblotted using antibodies anti-Reg1A (orb100720, Biorbyt) or Reg1B (E-AB-52897, Elabscience) (Figure S5I,K).

Immunohistochemical staining

Formalin-fixed paraffin-embedded (FFPE) duodenal 4 μm sections were utilized for immunohistochemical staining. Slides were deparaffinized in 100% Xylene and rehydrated in ethanol (100%, 96% and 70%) and H2O, following by block of endogenous peroxidase in 3% H2O2 methanol for 20 minutes and heat-induced epitope retrieval (HIER) in citrate buffer pH 6.0 at 98°C for 10 minutes in the Thermo Scientific PT Module. After incubation for 10 minutes with Ultravision protein block (Thermo Fisher Scientific, Breda, The Netherlands), FFPE sections were incubated with anti-Reg1B primary antibody (for Figure 6D,E: 1:100 dilution in TBS, MA5-29517, Invitrogen, Waltham, Massachusetts, USA) for 1 hour at room temperature (RT), following by incubation with the secondary antibodies BrightVision Poly-HRP-conjugates goat anti-rabbit IgG (undiluted) for 30 minutes. For assessing the expression and localization of Reg1B in duodenal tissue with different antibodies and to compare its expression to the one of Reg1A (Figure S5H), following 10-minutes HIER in citrate buffer, duodenal sections were incubated with primary antibodies against Reg1B (1:2000, E-AB-52897, Elabscience, Houston, USA) or against Reg1A (1:2000, orb100720, Biorbyt, Cambridge, UK). All single-stainings were visualized with 3,3'Diaminobenzidine (DAB) kit (Sigma Aldrich, Zwijndrecht, The Nederlands).

For the triple staining of REG1B, lysozyme and mucin were stained in sequential order using sequentially cut duodenal FFPE sections. Reg1B expression was visualized by: 10-minute HIER in citrate buffer pH 6.0 at 98°C, 1-hour incubation at RT with anti-Reg1B rabbit IgG (Invitrogen, MA5-29517, 1:100 dilution in TBS), 30-minute incubation with BrightVision Poly-alkaline phosphatase (AP)-conjugated goat anti-rabbit IgG (undiluted) and staining development with Perma Red/AP kit (Diagnostic BioSystem, Pleasanton, California, USA). Lysozyme (as marker of Paneth cells) was stained

following: 5-minute HIER in Tris-EDTA pH 9.0 buffer at 98°C, 30-minute incubation at RT with polyclonal rabbit anti-lysozyme (1:2000 dilution in TBS, Dako EC 3.2.1.17, Agilent Technologies, Santa Clara, California, USA), 30-minute incubation with BrightVision Poly-HRP-conjugated goat anti-rabbit IgG (1:2 dilution in TBS) and staining development with Perma Yellow/HRP kit (Diagnostic BioSystem). For the final detection of acidic mucins (to mark Goblet cells), FFPE double-stained slides were incubated with Alcian Blue solution (1% in 3% acetic acid, pH 2.5, Sigma Aldrich) for 5 minutes and eventually covered with coverslips using VectaMount mounting medium (Thermo Fisher Scientific, H-5000).

Cell culture and assay procedure

Caco-2 cells were cultured in Gibco Dulbecco's Modified Eagle Medium (DMEM) supplemented with 10% fetal bovine serum (FBS), 100 IU/ml penicillin, 100 IU/ml streptomycin, and 2mM glutamine (Thermo Fisher Scientific) in T75 flasks. The day prior to the stimulation assays, cells were seeded at $1x10^5$/well in a 12-well plates; after resting overnight, cells were exposed to 1mM butyrate or 1 µg/ml muramyl dipeptide (MDP) (both stock solutions diluted in water) for 6 hours. Afterwards cells were washed once in PBS and lysated in RIPA buffer. Reg1B concentrations were determined by ELISA (Cloud-Clone Corp., Uscn Life Science Kit Inc., Wuhan, China) accordingly to the manufacturer's instructions in Caco-2 cells exposed to increasing concentrations of *A. soehngenii* L2-7 cells (10^5/ml and 10^6/ml). Prior to use in cell culture, bacteria were heat-inactivated at 65°C for 20 minutes. BCA protein assay kit (Thermo Fisher) was used to assess protein concentrations.

Measurements of fecal SCFA and plasma SCFA, incretins, bile acids and Reg1B

Fecal SCFAs (butyrate, acetate, propionate) were measured in morning stool samples (N=11), directly frozen at -20°C after collection, using gas chromatography coupled to tandem mass spectrometry detection (GC-MS/MS) as described previously[14]. Briefly, approximately 20-100 mg of fecal samples were mixed with internal standards, added to glass vials and freeze dried. All samples were then acidified with HCl, and SCFAs were extracted with two rounds of diethyl ether extraction. The organic supernatant was collected, the derivatization agent N-tert-butyldimethylsilyl-N-methyltrifluoroacetamide (Sigma-Aldrich, Stockholm, Sweden) was added and samples were incubated at room temperature overnight. SCFAs were quantified with a gas chromatograph (Agilent Technologies 7890A, Santa Clara, California, USA) coupled to a mass spectrometer (Agilent Technologies 5975C). Short chain fatty acid standards were attained from Sigma-Aldrich (Stockholm, Sweden).

Plasma SCFA (butyrate, acetate, propionate) were measured at Cleveland Clinic (OH, USA) in heparin plasma samples (N=12), directly frozen at -80-°C after collection, using gas chromatography coupled to TANDEM mass spectrometry (GC-MS/MS) as previously described[15]. Briefly, 30 µl aliquots of plasma were mixed with 50 µl 2-Butanol/Pyridine (3:2) and 5 µl containing the heavy labeled internal

standards. Afterwards, the carboxylic acids were derivatized by mixing 50 µl supernatant with 10 µl isobutyl chloroformate, followed by vortexing and sonicating the mixture. After derivatization, 50 µl hexane were added and mixed; following centrifugation, the top hexane layer was removed for GC-MS/MS analysis and 1 µl was injected into GC column. The quantitation of butyric acid, acetic acid, and propionic acid was performed using isotope dilution GC-MS/MS and the absolute concentration of each SCFA was determined using calibrations curves measured for each analyte. Samples were analyzed on a Thermo TSQ-Evo triple quadrupole mass spectrometer interfaced with the Trace 1310 gas chromatograph (Thermo Fisher Scientific). Chromatographic separation was achieved by using an HP-5MS fused-silica capillary column (30 m × 0.250 mm × 0.25 µm; Agilent Technologies, Santa Clara, CA, USA) coated with 5% phenymethyl siloxane as previously described[15]. The mass spectrometer was used in MRM mode with the following parent to daughter ion transitions: m/z 61.0 → 43.0 for acetic acid, m/z 63.0 → 45.0 for [13C2]-acetic acid, m/z 61.0 → 43.0 m/z 71.0 → 41.0 for butyric acid, m/z 78.1 → 46.1 for D7-butyric acid, m/z 75.1 → 57.0 for propionic acid, m/z 77.1 → 59.0 for D2-propionic acid.

Plasma incretin levels of all 12 individuals were determined in postprandial (2-hour mixed meal test) samples as previously described[16]. Plasma concentrations of GIP (total) and GLP-1 (total) were measured by Holst group with ELISA (cat no. 10-1258-01 and 10-1278-01, Mercodia, Sweden). All quality controls provided by the manufacturer were within allowed limits. All samples from the same individual were measured in the same assay run.

Concentrations of the secondary bile acids tauro-omega-muricholic acid (TOMCA), tauroursodeoxycholic acid (TUDCA), taurodeoxycholic acid (TDCA), tauroursodeoxycholic acid (TUDCA), taurolithocholic acid (TLCA), glycohyodeoxycholic acid (GHDCA), glycodeoxycholic acid (GDCA), glycoursodeoxycholic acid (GUDCA), glycolithocholic acid (GLCA), omega-muricholic acid (OMCA), deoxycholic acid (DCA), ursodeoxycholic acid (UDCA), lithocholic acid (LCA), hyodeoxycholic acid (HDCA), murocholic acid (MuroCA), iso-ursodeoxycholic acid (IsoUDCA) were measured in plasma samples from all 12 participants by means of ultra-performance liquid chromatography-tandem mass spectrometry (UPLCMS/MS), as previously performed[17]. Briefly, samples (50µl) were extracted with 10 volumes of methanol containing deuterated internal standards (d_4-TCA, d_4-GCA, d_4-GCDCA, d_4-GUDCA, d_4-GLCA, d_4-UDCA, d_4-CDCA, d_4-LCA; 50nM of each). After 10 minutes of vortex and 10 minutes of centrifugation at 20 000g, the supernatant was evaporated under a stream of nitrogen and reconstituted in 200µl methanol:water [1:1]. The samples were injected (5µl) and bile acids were separated on a C18 column (1.7µ, 2.1 x 100mm; Kinetex, Phenomenex, USA) using water with 7.5mM ammonium acetate and 0.019% formic acid (mobile phase A) and acetonitrile with 0.1% formic acid (mobile phase B). The chromatographic separation started with 1 minute isocratic separation at 20%B. The B-phase was then increased to 35% during 4 minutes. During the next 10 minutes the B-phase was increased to 100%. The B-phase was held at 100% for 3.5 minutes before

returning to 20%. The total runtime was 20 minutes. Bile acids were detected using multiple reaction monitoring (MRM) in negative mode on a QTRAP 5500 mass spectrometer (Sciex, Concord, Canada) and quantification was made using external standard curves.

Concentrations of Reg1B in plasma samples and duodenal tissue lysates was assessed by ELISA (Cloud-Clone Corp., Uscn Life Science Kit Inc., Wuhan, China) accordingly to the manufacturer's instructions.

Strain-specific qPCR

The DNA concentrations were determined fluorometrically (Qubit dsDNA HS assay; Invitrogen) and adjusted to 1 ng/µl prior to use as the template in qPCR. Primers targeting 16S rRNA gene of *A. soehngenii* L2-7 EhalF (5'GCGTAGGTGGCAGTGCAA) and EhalR (5'GCACCGRAGCCTATACGG) (Ramirez et al. 2008) were used for quantification. Standard template DNA was prepared from the 16S rRNA gene of *A. soehngenii* L2-7 by amplification with primers 27F (5'-AGAGTTTGATCCTGGCTCAG-3') and 1492R (5'-GGTTACCTTGTTACGACTT-3'). Standard curves were prepared with nine standard concentrations of 100 to 10^8 gene copies/µl. PCRs were performed in triplicate with iQ SYBR Green Supermix (Bio-Rad) in a total volume of 10 µl with primers at 500 nM in 384-well plates sealed with optical sealing tape. Amplification was performed with an iCycler (Bio-Rad, USA) with the following protocol: one cycle of 95°C for 10 min; 40 cycles of 95°C for 15 s, 55°C for 20 s, and 72°C for 30 s each; one cycle of 95°C for 1 min, one cycle of 60°C for 1 min, and a stepwise increase of the temperature from 60 to 95°C (at 0.5°C per 5 s) to obtain melt curve data. Data were analysed using the Bio-Rad CFX Manager 3.0.

Fecal 16S rRNA gene amplicon sequencing and bioinformatics

DNA extraction from fecal samples from 11 patients was performed using the repeated bead beating protocol as previously described[18]. DNA was eluted in 50 µl of DNAse- RNAse-free water and its concentration and quality were evaluated using NanoDrop 2000 spectrophotometry. Subsequently, DNA was diluted to reach a concentration of 20 ng/µl which served as template for PCR. The V5-V6 region of 16S ribosomal RNA (rRNA) gene was amplified in duplicate PCR reactions for each sample in a total reaction volume of 50 µl using a master mix containing 1 µl of a unique barcoded primer, 784F-n and 1064R-n (10 µM each per reaction), 1 µl dNTPs mixture, 0.5 µl Phusion Green Hot Start II High-Fidelity DNA Polymerase (2 U/µl; Thermo Scientific, Landsmeer, The Netherlands), 10 µl 5× Phusion Green HF Buffer, and 36.5 µl DNAse- RNAse-free water[19]. The amplification program included 30 seconds (s) of initial denaturation step at 98°C, followed by 25 cycles of denaturation at 98°C for 10 s, annealing at 42°C for 10 s, elongation at 72°C for 10 s, and a final extension step at 72°C for 7 minutes. The PCR product was visualized on 1% agarose gel (~280 bp) and purified with CleanPCR kit (CleanNA, Alphen aan den Rijn, The Netherlands). The concentration of the purified PCR product was measured with Qubit dsDNA BR Assay Kit (Invitrogen, California, USA) and 200 ng of microbial

DNA from each sample were pooled for the creation of the final amplicon library which was sequenced (150 bp, paired-end) on the Illumina HiSeq 2500 platform (GATC Biotech, Constance, Germany).

Raw reads were demultiplexed using the Je software suite (v2.0)[20] allowing no mismatches in the barcodes. After removing the barcodes, linker and primers, reads were mapped against the human genome using bowtie2 (v2.4.1)[21] in order to remove human reads. Surviving microbial forward and reverse reads were pipelined separately using DADA2 (v1.12.1)[22]. Amplicon Sequence Variants (AVSs) inferred from the reverse reads were reverse-complemented and matched against ASVs inferred from the forwards reads. Only non-chimeric forward reads ASVs that matched reverse-complemented reverse reads ASVs were kept. ASV sample counts were inferred from the forward reads. ASV taxonomy was assigned using DADA2 and the SILVA (v132) database. The resulting ASV table and taxonomy assignments were integrated using the phyloseq R package (v1.28.0)[23]. ASVs sequences were aligned using MAFFT (v.7.427)[24] using the auto settings. A phylogenetic tree was constructed from the resulting multiple sequence alignment with FastTree (v.2.1.11 Double Precision)[25] using a generalized time-reversible model ('-gtr'). Biopsy samples were rarefied to 24947 counts per sample, while fecal samples were rarefied to 13229 counts per sample. The vegan R package (v2.5.6)[26] was used to calculate alpha-diversity metrics (Shannon index and ASV richness) and Bray-Curtis dissimilarities. Weighted-Unifrac distances were calculated using the phyloseq package.

Power calculation and statistical analyses

We based our power calculation on the study of Van Baarlen *et al.*[27], in which a striking difference in duodenal mucosal transcriptomic profiling was reported 6 hours after introduction of a single *Lactobacillus* bacterial strain. Based on 60% decrease in duodenal *Fxr* gene expression upon *A. soehngenii* L2-7 administration to db/db mice, compared to placebo[18], with one sample Chi^2 test, the sample size in each group needed to be 12 in order to have a group proportion of 0.5 and with a comparison proportion of 0.1. Mean absolute deviation of glucose (MAD), continuously measured using FreeStyle Libre technology, was calculated using the default 'mad' function from R stats package[28]. Wilcoxon signed rank tests and Mann-Whitney U-tests were used to compare within-group changes of related samples and to compare intervention groups. Student's t-test was used for analyzing differences in groups from *in vitro* experiments. Area under the curve (AUCs) for MMT measurement were calculated using the DescTools package (v0.99.36) [29,30]. Correlation plots were made using the corrplot package (v0.84) [31]. The mixOmics package (v6.12.1) [32] was used to perform multilevel PCA analyses. Principal Coordinate Analyses (PCoA) were performed using the ape package (v5.4)[33]. All other statistical analyses and visualizations were performed in R (v4.0.1)[34] using the tidyverse (v1.3.0)[35] and ggplot2 package (v3.3.1)[30]. P values <0.05 were considered statistically significant.

SI References

1. Gilijamse, P. W. *et al.* Treatment with Anaerobutyricum soehngenii: a pilot study of safety and dose–response effects on glucose metabolism in human subjects with metabolic syndrome. *npj Biofilms Microbiomes* **6**, 1–10 (2020).

2. Andrews, S. FastQC: a quality control tool for high throughput sequence data. (2015).

3. Bolger, A. M., Lohse, M. & Usadel, B. Trimmomatic: a flexible trimmer for Illumina sequence data. *Bioinformatics* **30**, 2114–2120 (2014).

4. Bray, N. L., Pimentel, H., Melsted, P. & Pachter, L. Near-optimal probabilistic RNA-seq quantification. *Nat. Biotechnol.* **34**, 525–527 (2016).

5. Pimentel, H., Bray, N. L., Puente, S., Melsted, P. & Pachter, L. Differential analysis of RNA-seq incorporating quantification uncertainty. *Nat. Methods* **14**, 687–690 (2017).

6. Love, M. I., Huber, W. & Anders, S. Moderated estimation of fold change and dispersion for RNA-seq data with DESeq2. *Genome Biol.* **15**, 550 (2014).

7. Robinson, M. D., McCarthy, D. J. & Smyth, G. K. edgeR: a Bioconductor package for differential expression analysis of digital gene expression data. *Bioinformatics* **26**, 139–140 (2010).

8. Robinson, M., Mccarthy, D., Chen, Y., Lun, A. & Smyth, G. K. edgeR: differential expression analysis of digital gene expression data. (2012).

9. Fernandes, A. D. *et al.* Unifying the analysis of high-throughput sequencing datasets: characterizing RNA-seq, 16S rRNA gene sequencing and selective growth experiments by compositional data analysis. *Microbiome* **2**, 15 (2014).

10. McCarthy, D. J., Chen, Y. & Smyth, G. K. Differential expression analysis of multifactor RNA-Seq experiments with respect to biological variation. *Nucleic Acids Res.* **40**, 4288–4297 (2012).

11. Soneson, C., Love, M. I. & Robinson, M. D. Differential analyses for RNA-seq: transcript-level estimates improve gene-level inferences. *F1000Research* **4**, 1521 (2015).

12. Durinck, S., Spellman, P. T., Birney, E. & Huber, W. Mapping identifiers for the integration of genomic datasets with the R/Bioconductor package biomaRt. *Nat. Protoc.* **4**, 1184 (2009).

13. Benjamini, Y. & Hochberg, Y. Controlling the false discovery rate: a practical and powerful approach to multiple testing. *J. R. Stat. Soc. Ser. B* 289–300 (1995).

14. Wichmann, A. *et al.* Microbial modulation of energy availability in the colon regulates intestinal transit. *Cell Host Microbe* **14**, 582–590 (2013).

15. Arnon D Lieber, AD. et al. Loss of HDAC6 alters gut microbiota and worsens obesity. FASEB J 33(1), 1098-1109 (2019).

16. Kootte, R. S. *et al.* Improvement of Insulin Sensitivity after Lean Donor Feces in Metabolic Syndrome Is Driven by Baseline Intestinal Microbiota Composition. *Cell Metab.* (2017). doi:10.1016/j.cmet.2017.09.008

17. Tremaroli, V. *et al.* Roux-en-Y Gastric Bypass and Vertical Banded Gastroplasty Induce Long-Term Changes on the Human Gut Microbiome Contributing to Fat Mass Regulation. *Cell Metab.* **22**, 228–238 (2015).

18. Salonen, A. *et al.* Comparative analysis of fecal DNA extraction methods with phylogenetic microarray: Effective recovery of bacterial and archaeal DNA using mechanical cell lysis. *J.*

Microbiol. Methods **81**, 127–134 (2010).

19. Ramiro-Garcia, J. *et al.* NG-Tax, a highly accurate and validated pipeline for analysis of 16S rRNA amplicons from complex biomes. *F1000Research* **5**, 1791 (2016).

20. Girardot, C., Scholtalbers, J., Sauer, S., Su, S.-Y. & Furlong, E. E. M. Je, a versatile suite to handle multiplexed NGS libraries with unique molecular identifiers. *BMC Bioinformatics* **17**, 419 (2016).

21. Langmead, B. & Salzberg, S. L. Fast gapped-read alignment with Bowtie 2. *Nat. Methods* **9**, 357 (2012).

22. Callahan, B. J. *et al.* DADA2: High-resolution sample inference from Illumina amplicon data. *Nat Meth* **13**, 581–583 (2016).

23. McMurdie, P. J. & Holmes, S. phyloseq: An R Package for Reproducible Interactive Analysis and Graphics of Microbiome Census Data. *PLoS One* **8**, e61217 (2013).

24. Katoh, K., Misawa, K., Kuma, K. & Miyata, T. MAFFT: a novel method for rapid multiple sequence alignment based on fast Fourier transform. *Nucleic Acids Res.* **30**, 3059–66 (2002).

25. Price, M. N., Dehal, P. S. & Arkin, A. P. FastTree 2 - Approximately maximum-likelihood trees for large alignments. *PLoS One* **5**, e9490 (2010).

26. Oksanen, J. *et al.* vegan: Community Ecology Package. (2017).

27. van Baarlen, P. *et al.* Differential NF- B pathways induction by Lactobacillus plantarum in the duodenum of healthy humans correlating with immune tolerance. *Proc. Natl. Acad. Sci.* **106**, 2371–2376 (2009).

28. Fokkert, M. J. *et al.* Performance of the freestyle libre flash glucose monitoring system in patients with type 1 and 2 diabetes mellitus. *BMJ Open Diabetes Res. Care* **5**, 1–8 (2017).

29. Signorell, A. DescTools: Tools for Descriptive Statistics. (2020).

30. Wickham, H. *ggplot2: Elegant Graphics for Data Analysis*. (Springer-Verlag New York, 2016).

31. Wei, T. & Simko, V. R package 'corrplot': visualization of a correlation matrix (version 0.84).'. *Retrived from https//github. com/taiyun/corrplot* (2017).

32. Cao, K.-A. Le, Rohart, F., Gonzalez, I. & Dejean, S. mixOmics: Omics Data Integration Project, package version 6.1.2 https://CRAN.R-project.org/package=mixOmics. (2017).

33. Paradis, E. & Schliep, K. ape 5.0: an environment for modern phylogenetics and evolutionary analyses in R. *Bioinformatics* **35**, 526–528 (2019).

34. R Core Team. R: A language and environment for statistical computing. R Foundation for Statistical Computing. (2016).

35. Wickham, H. *et al.* Welcome to the Tidyverse. *J. Open Source Softw.* **4**, 1686 (2019).

SI Legends of Figures and Tables

Figure S1: Fecal *A. soehngenii* L2-7 levels

Fecal *A. soehngenii* L2-7 levels determined by qPCR at 0, 24 hours, 1 week, 2 weeks after placebo/treatment-interventions. Values indicate gene copies per gr of feces.

Figure S2: Fecal short-chain fatty acids

(A) Concentrations (nmol/mg dried feces weight) of butyrate, (**B**) acetate, and (**C**) propionate in morning stool samples obtained at baseline and 1 day after placebo/treatment-intervention.

Figure S3: Postprandial glucose and insulin
(**A**) Plasma glucose levels (mmol/l) at 0, 20, 30, 120 minutes during mixed meal test (MMT). (**B**) Plasma glucose levels during MMT as total area under the curve (AUC). (**C**) Plasma insulin levels (pmol/l) at 0, 20, 30, 120 minutes during MMT. (**D**) Plasma insulin levels during MMT as total area under the curve (AUC).

Figure S4: Plasma short-chain fatty acids

(A) Concentrations (μM) of butyrate, (**B**) acetate, and (**C**) propionate in plasma at 120 minutes of mixed meal test (MMT).

Figure S5: Duodenal expression of REG genes and Reg1A/1B proteins

Gene expression measured by qPCR in duodenal biopsies at 6 hours post-intervention of (**A**) *REG1B* (different set of forward and reverse primers than in Figure 6B), (**B**) *REG3A*, (**C**) *REG3G*, and (**D**) *REG4*. (**A-D**) Data showing the relative gene expression (to placebo) using the 2ˆ-(delta delta Ct) method. (**E**) Quantification of Reg1A expression levels in duodenal biopsies, Reg1A expression normalized to β-actin (loading control). (**F**) Reg1A expression shown as fold-change treatment versus placebo. (**G**) Westernblot images of duodenal lysates blotted with antibodies against Reg1A and β-actin. (**H**) Immunohistochemical staining of Reg1B (different antibodies used than in Figures 6D,6E) and Reg1A in duodenal biopsies. (**I,K**) Westernblot images showing the specificity of the antibodies against Reg1B and Reg1A; (**I**) Westernblotting for Reg1B: enhanced band intensity with increasing amount of loaded recombinant human (rh)Reg1B and absence of a band when rh Reg1A is loaded; ; (**K**) Westernblotting for Reg1A: stronger band intensity with increasing amount of loaded rh Reg1A and absence of a band when rh Reg1B is loaded. (**J**) Circulating levels (ng/ml) of Reg1B measured by ELISA in plasma samples taken at 8 hours post-intervention. (**L**) Reg1b expression by Caco-2 cells in response to exposure to increasing concentrations of heat-inactivated *A. soehngenii* L2-7 cells.

Figure S6: Assessment of carry-over affect between week 0 and week 4

(**A**) Fecal *A. soehngenii* L2-7 levels determined by qPCR at baseline (week 0 and week 4); values indicate gene copies per gr of feces. (**B**) Concentrations (nmol/mg dried feces weight) of butyrate in morning stool samples obtained at baseline (week 0 and week 4). (**C**) Plasma GLP-1 levels during mixed meal test (MMT) shown as total area under the curve (AUC). (**D**) Median absolute deviation (MAD) of continuous glucose measurements (CGM) over the first 24 hours after placebo/treatment-intervention.

Table S1: Baseline characteristics and safety parameters at both study visits

Data expressed as medians and interquartile ranges. There were no differences after the *A. Soehngenii* L2-7 infusion compared to the placebo infusion. BMI: body mass index, HOMA-IR: homeostatic model assessment of insulin resistance, HbA1c: glycated hemoglobin, HDL: high-density lipoprotein, LDL: low-density lipoprotein; AST: aspartate transaminase, ALT: alanine transaminase, AP: alkaline phosphatase; γgt: gamma-glutamyltransferase; CRP: c-reactive protein.

Table S2

Primer sequences utilized in the analysis of duodenal gene expression. *: primers used in Figure S5A.

Koopen A, *et al. Gut* 2022;0:1–11. doi: 10.1136/gutjnl-2020-323297

Table S1

	Placebo	A. Soehngenii	P - value
Weight (kg)	110.1 [100.0 – 120.2]	110.4 [101.3 – 122.0]	0.812
BMI (kg/m2)	33.4 [32.2 – 38.]	33.7 [31.8 – 37.8]	0.859
Blood pressure: systolic (mmHg)	135 [129 – 147]	144 [131 – 156]	0.258
Blood pressure: diastolic (mmHg)	89 [84 – 91)	91 [79 – 95)	0.917
Fasting glucose (mmol/L)	5.3 [5.0 – 5.6]	5.1 [4.8 – 5.7]	0.430
Insulin (pmol/L)	65 [48 – 83]	56 [34 – 81]	0.099
HOMA - IR	2.3 [1.7 – 2.8]	1.9 [1.1 – 2.8]	0.158
HbA1c (mmol/mol)	37 [36 – 39]	37 [36 – 39]	0.942
Cholesterol: total (mmol/L)	5.29 [4.57 – 6.26]	5.13 [4.71 – 6.08]	0.255
Cholesterol: HDL (mmol/L)	1.17 [0.91 – 1.31]	1.13 [0.97 – 1.32]	0.929
Cholesterol: LDL (mmol/L)	3.05 [2.69 - 3.90]	3.21 [2.79 – 3.83]	0.638
Cholesterol: triglycerides (mmol/L)	1.65 [1.12 – 2.92]	1.66 [1.19 – 2.31]	0.433
Creatinine (umol/L)	87 [78 – 92]	84 [79 – 93]	0.342
AST (U/L)	25 [19 – 31]	26 [23 – 33]	0.109
ALT (U/L)	25 [21 – 36]	27 [22 – 35]	0.124
AP (U/L)	70 [62 – 85]	72 [60 -87]	0.783
yGT (U/L)	39 [26 – 52]	31 [26 – 49]	0.254
CRP (mg/ml)	2.8 [1.8 – 5.0]	3.0 [2.3 – 5.3]	0.477
Leukocytes (10^e9/L)	6.2 [5.6 – 6.7]	6.5 [5.9 – 7.3]	0.130
Caloric intake (kcal/day)	1843 [1607 – 2090]	1888 [1667 – 2041]	0.424
Fat intake (g)	68 [57 – 75]	61 [56 – 81]	0.790
Protein intake (g)	76 [65 – 85]	77 [60 – 91]	0.333
Carbohydrate intake (g)	201 [162 – 233]	228 [173 – 254]	0.241
Fiber intake (g)	18 [14 – 19]	19 [16 – 21]	0.339

Koopen A, *et al. Gut* 2022;0:1–11. doi: 10.1136/gutjnl-2020-323297

Table S2

Gene	Forward primer sequence	Reverse primer sequence
GPR43/FFAR2	TGCTACGAGAACTTCACCGAT	GGAGAGCATGATCCACACAAAAC
TGR5	CACTGTTGTCCCTCCTCTCC	ACACTGCTTTGGCTGCTTG
FXR	TACATGCGAAGAAAGTGTCAAGA	ACTGTCTTCATTCACGGTCTGAT
FGF19	CGGAGGAAGACTGTGCTTTCG	CTCGGATCGGTACACATTGTAG
OSTalpha	CTGGGCTCCATTGCCATCTT	CACGGCATAAAACGAGGTGAT
REG1B	GGTCCCTGGTCTCCTACAAG	TCCATTTCTTGAATCCTGAGCA
REG1A	GGTCCCTGGTCTCCTACAAG	CATTTCTGGAATCCTGTGCTTG
REG1B*	AGTAGTGGGTCCCTGGTCTC	TGAATCCTGAGCATGAAGTCA
REG3A	AGCTACTCATACGTCTGGATTGG	CACCTCAGAAATGCTGTGCTT
REG3G	GGTGAGGAGCATTAGTAACAGC	CCAGGGTTTAAGATGGTGGAGG
REG4	CTGCTCCTATTGCTGAGCTG	GGACTTGTGGTAAAACCATCCAG
ACTB	CCAACCGCGAGAAGATGA	CCAGAGGCGTACAGGGATAG

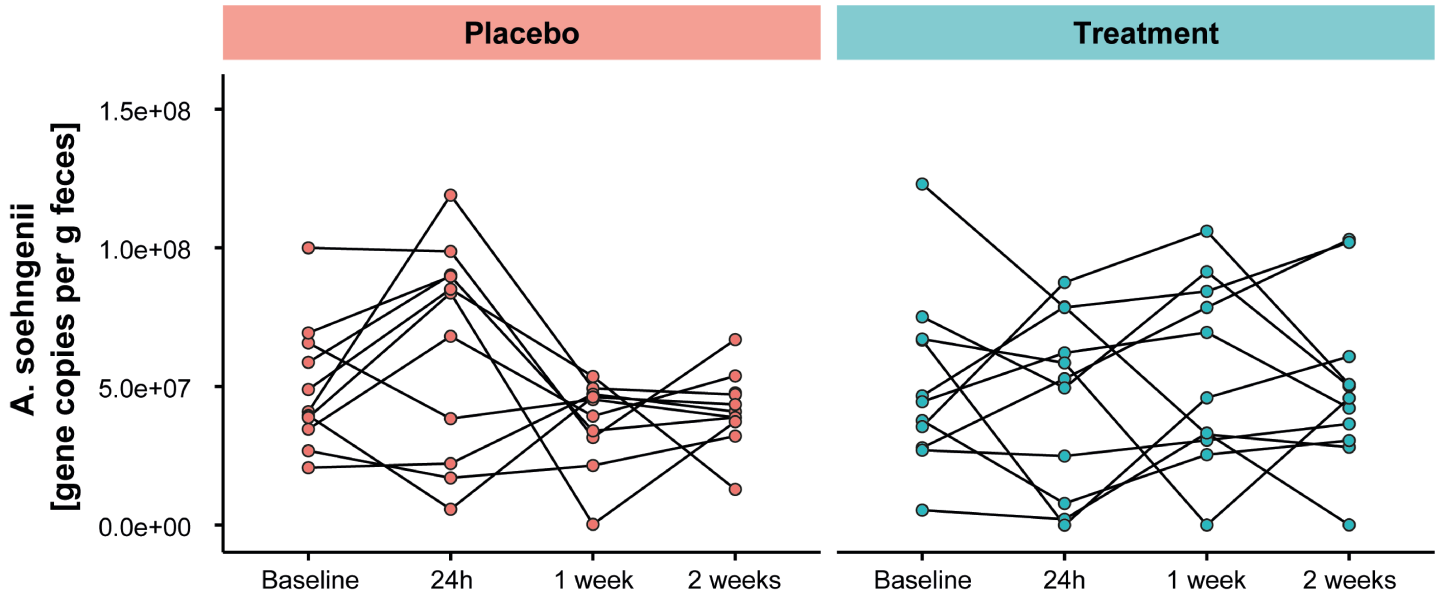
Placebo
Treatment
A. soehngenii
[gene copies per g feces]
1.5e+08
1.0e+08
5.0e+07
0.0e+00
Baseline
24h
1 week
2 weeks
Baseline
24h
1 week
2 weeks

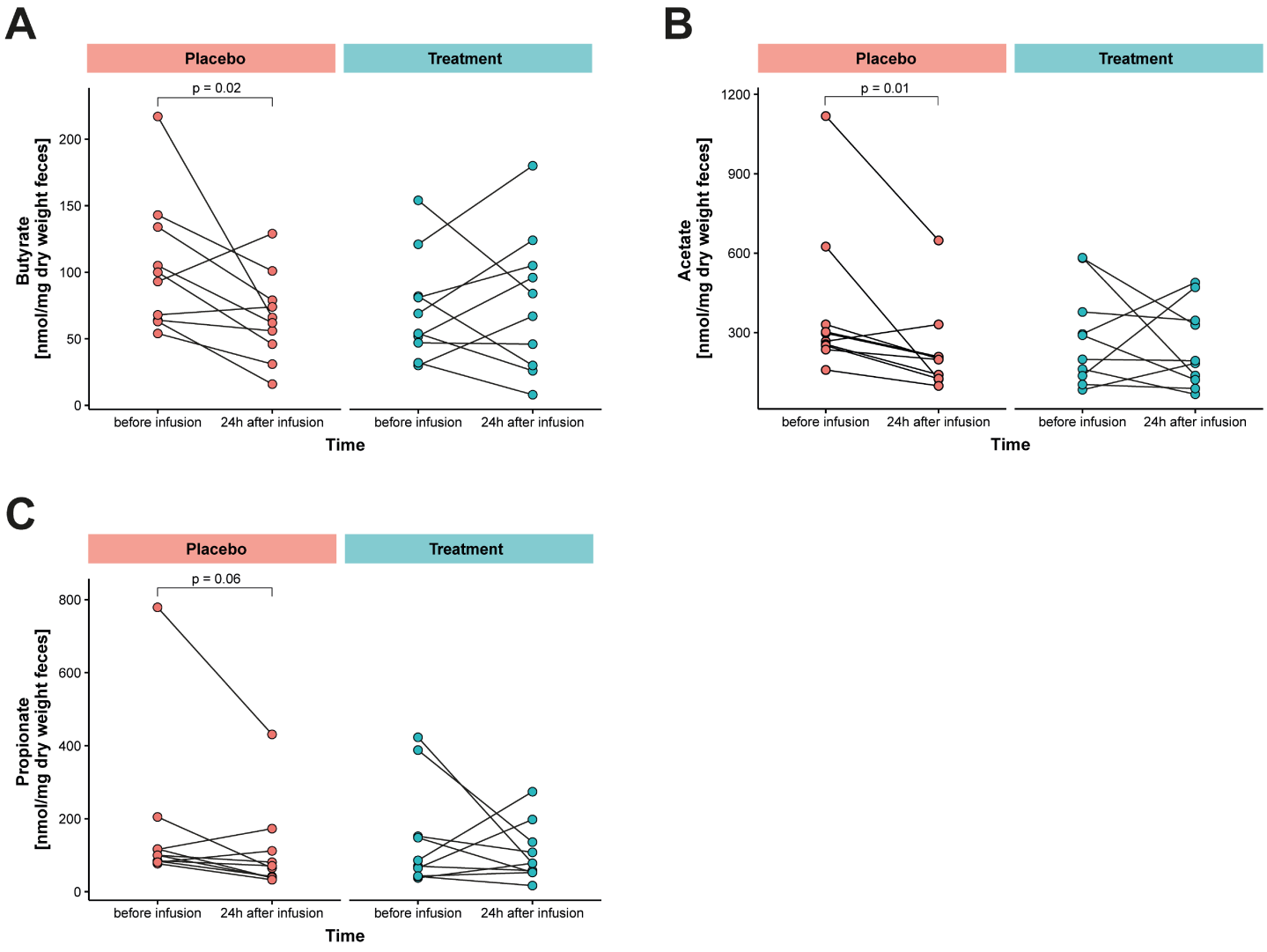
A
Placebo
Treatment
p = 0.02
Butyrate
[nmol/mg dry weight feces]
0
50
100
150
200
before infusion
24h after infusion
Time
B
Placebo
Treatment
p = 0.01
Acetate
[nmol/mg dry weight feces]
300
600
900
1200
before infusion
24h after infusion
Time
C
Placebo
Treatment
p = 0.06
Propionate
[nmol/mg dry weight feces]
0
200
400
600
800
before infusion
24h after infusion
Time

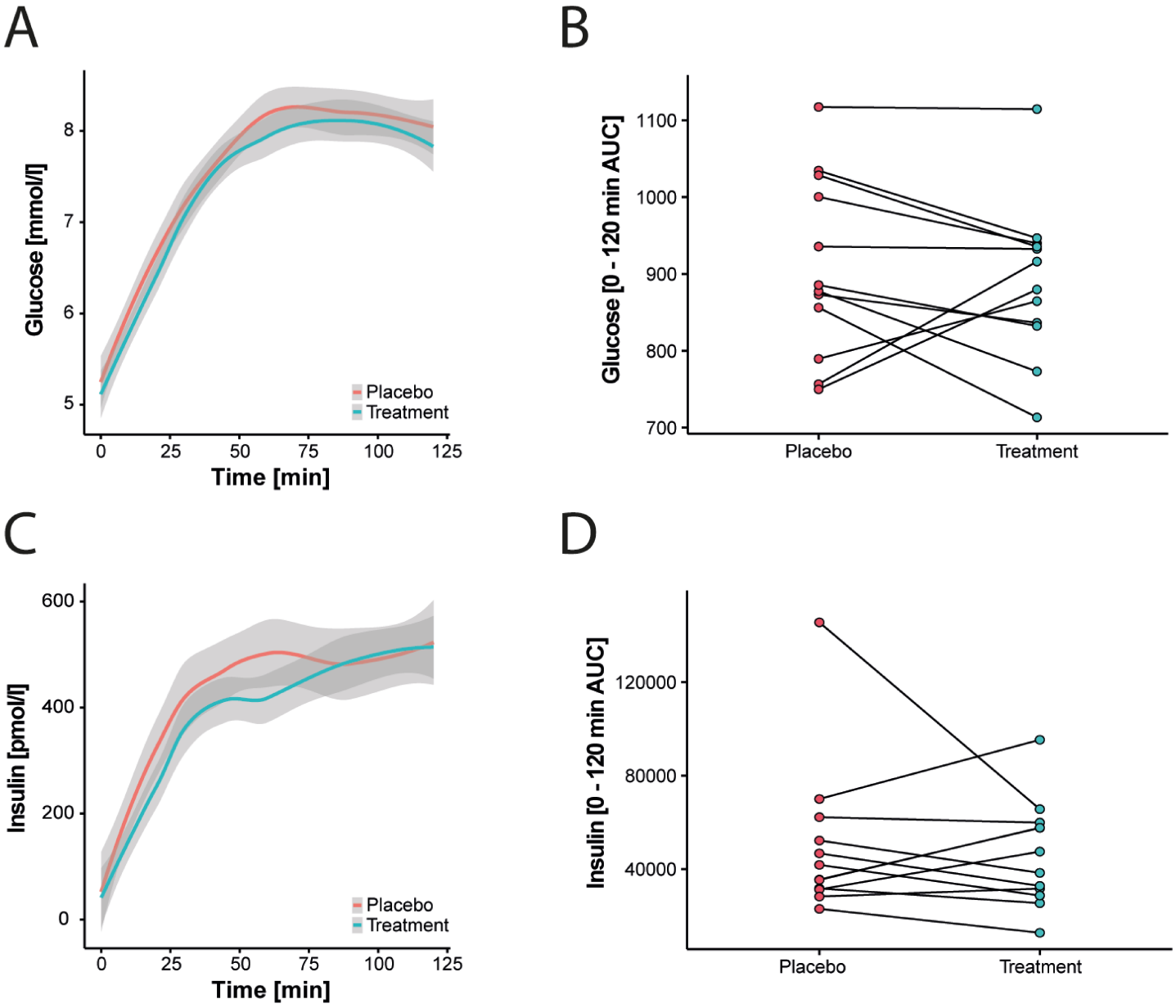
A
Glucose [mmol/l]
8
7
6
5
0
25
50
75
100
125
Time [min]
Placebo
Treatment
B
Glucose [0 - 120 min AUC]
1100
1000
900
800
700
Placebo
Treatment
C
Insulin [pmol/l]
600
400
200
0
0
25
50
75
100
125
Time [min]
Placebo
Treatment
D
Insulin [0 - 120 min AUC]
120000
80000
40000
Placebo
Treatment

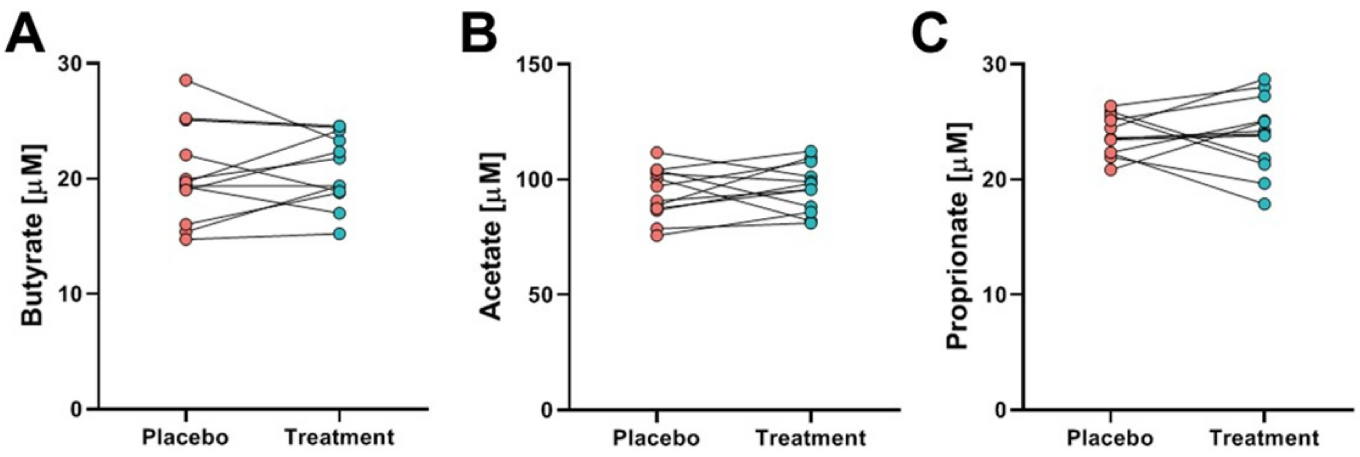
A
Butyrate [µM]
30
20
10
0
Placebo
Treatment
B
Acetate [µM]
150
100
50
0
Placebo
Treatment
C
Proprionate [µM]
30
20
10
0
Placebo
Treatment

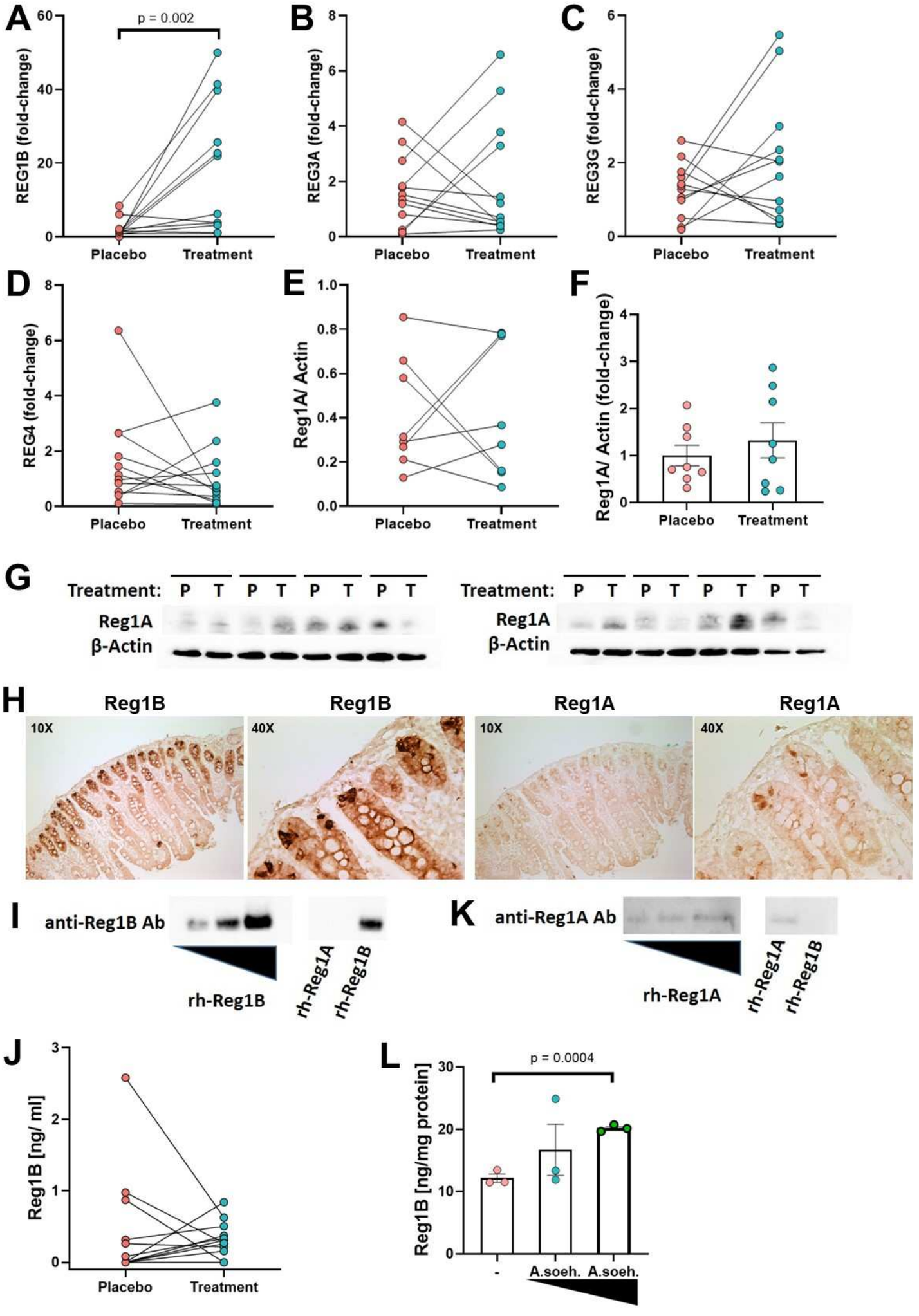
A
p = 0.002
REG1B (fold-change)
Placebo
Treatment
B
REG3A (fold-change)
C
REG3G (fold-change)
D
REG4 (fold-change)
E
Reg1A/ Actin
F
Reg1A/ Actin (fold-change)
G
Treatment: P T P T P T P T
Reg1A
β-Actin
H
Reg1B
Reg1A
10X
40X
I
anti-Reg1B Ab
rh-Reg1B
rh-Reg1A
rh-Reg1B
K
anti-Reg1A Ab
rh-Reg1A
J
Reg1B [ng/ ml]
L
p = 0.0004
Reg1B [ng/mg protein]
-
A.soeh.
A.soeh.

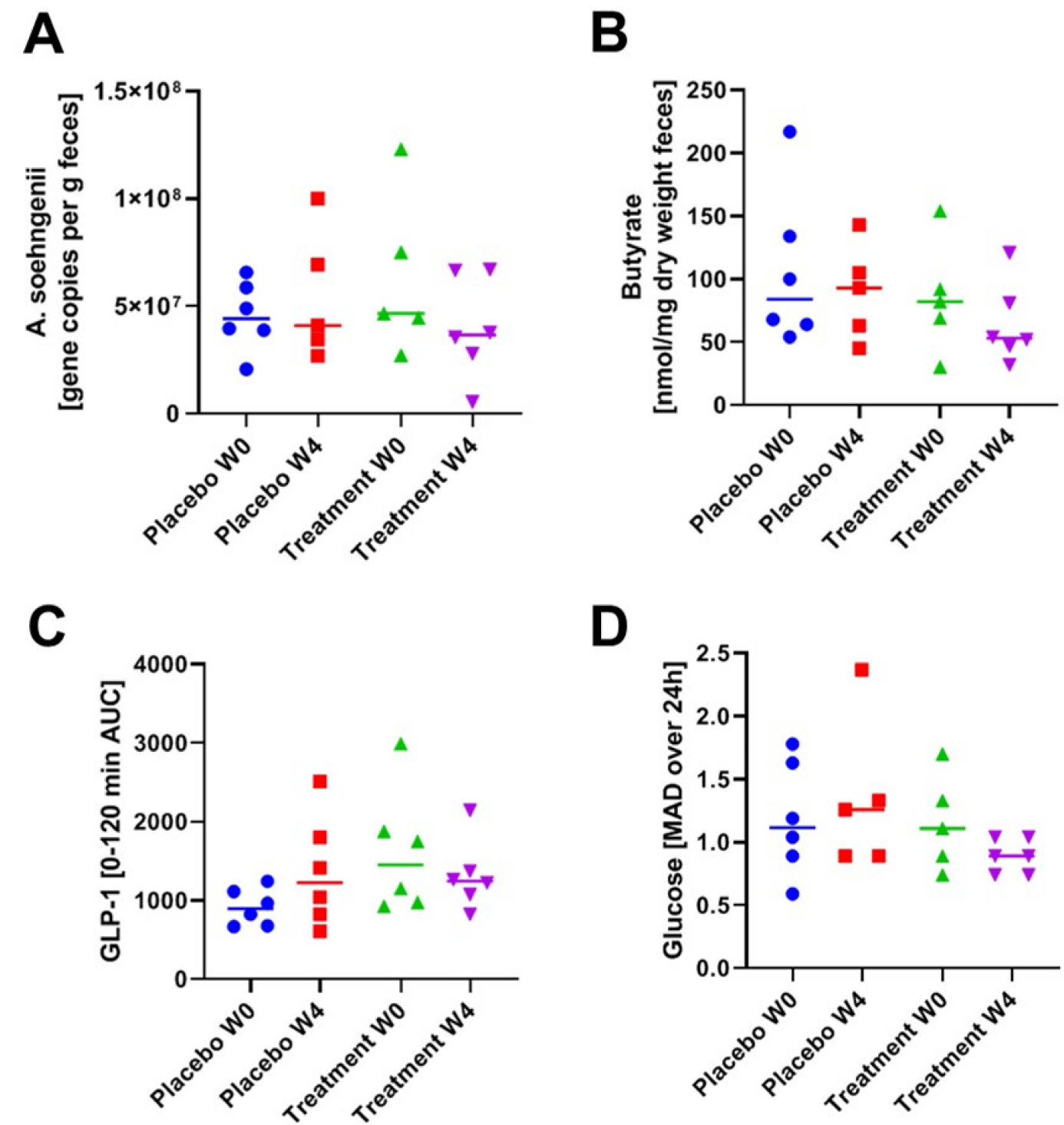
A
A. soehngenii [gene copies per g feces]
1.5×10⁸
1×10⁸
5×10⁷
0
Placebo W0
Placebo W4
Treatment W0
Treatment W4
B
Butyrate [nmol/mg dry weight feces]
250
200
150
100
50
0
Placebo W0
Placebo W4
Treatment W0
Treatment W4
C
GLP-1 [0-120 min AUC]
4000
3000
2000
1000
0
Placebo W0
Placebo W4
Treatment W0
Treatment W4
D
Glucose [MAD over 24h]
2.5
2.0
1.5
1.0
0.5
0.0
Placebo W0
Placebo W4
Treatment W0
Treatment W4

Supplementary Material (Supplementary Material and Methods and Supplementary Figures) for:

Duodenal *Anaerobutyricum soehngenii* infusion stimulates GLP-1 production, ameliorates glycemic control and beneficially shapes the duodenal transcriptome in metabolic syndrome subjects; a randomized double-blind placebo-controlled cross-over study.

Supplementary Material and Methods

Culturing of *A. soehngenii*

The cells were obtained as described previously[1] by culturing *A. soehngenii L2-7* at 500-liter scale in a basic phosphate-bicarbonate salt medium containing 2% yeast extract, 0.4% soy peptone, and 2% sucrose, at pH 6.8 and 37C. Following autoclaving, filter-sterilized components were added, including cysteine (final concentration 0.05%) and a 1 ml per liter of a vitamin solution (containing per liter 10 mg biotin, 10 mg cobalamin, 30 mg para-aminobenzoic acid, 50 mg folic acid, and 150 mg pyridoxamine). *A. soehngenii* L2-7 cells were harvested by microfiltration, washed with PBS, and finally stored in PBS containing 10% glycerol at a concentration of 10^{10} cells/ml in 10 ml tubes at -80°C. *A. soehngenii* L2-7 was handled under strict anaerobic conditions which were maintained during all stages of the production of the concentrated cells: during growth, microfiltration, glycerol mixing, and filling of the tubes with a nitrogen atmosphere. The viability of *A. soehngenii* L2-7 in randomly selected tubes (stored at -80°C at the AMC Department of Clinical Pharmacy) was tested every 6 months during the study using most probable number (MPN) analysis in YCFA medium. MPN analyses were performed in duplicate in anoxic YCFA medium containing sucrose incubated at 37°C for 5 days[1]. Growth was scored by visual and microscopic inspection. Viability stayed constant at 10^{10} cells/ml during the time of the study.

Duodenal RNA sequencing and differential gene expression analysis

RNA for RNA sequencing analysis was isolated from duodenum biopsies, which were directly snap-frozen in liquid nitrogen after biopsy and stored at -80˚C until analysis, from all 12 included participants, using an RNA isolation protocol optimized for small tissue biopsies. In short, biopsies were mixed with 300 µl TriPure (Roche, Basel, Switzerland) and homogenized on ice using a sterile, RNAse free pestle. After short centrifugation, 60 µl of chloroform was added. Samples were then added to a Heavy Phase Lock gel tube (Quanta Bio, Beverly, USA) and centrifuged (15 min, 12.000 x g, 4˚C). The aqueous phase was transferred and mixed with 1 volume of 70% ethanol. The mixture was added to a RNeasy MinElute spin column (QIAgen, Tegelen, the Netherlands). RNA was washed according to manufacturer's protocol and eluted in 14 µl RNAse free water. RNA concentration was measured using the NanoDrop 1000 (Thermo Scientific, Landsmeer, the Netherlands). RIN scores were assessed on a Bioanalyzer 2100 using Eukaryote Total RNA Nano chips (Agilent Technologies, Santa

Clara, USA). RNA was depleted from rRNA and sequenced on a HiSeq4000 (paired-end, 150 bp) by Genomescan BV, Amsterdam, The Netherlands.

RNA raw sequence quality was checked using FastQC (v0.11.9)[2] and quality trimmed and filtered using Trimmomatic (v0.38)[3]. The single, 50 bp reads were processed by removing the first 5 bases, applying a sliding-window quality trim 4 bp wide with a threshold of Q15, then removing all reads shorter than 36 bp after trimming. Quality checked and trimmed reads were subsequently pseudo aligned to the human transcriptome (GRCh38 release 97) using Kallisto (v0.46.0)[4]. The transcript-level counts from Kallisto output were used to perform differential gene expression analysis using 3 different R packages: sleuth (v0.30.0)[5], DESeq2 (v1.28.1)[6], and edgeR (v3.30.3)[7–10]. Count data was imported to DESeq2 and edgeR using the tximport package[11]. Transcript to gene mappings were obtained using the biomaRt package (v2.44.0)[12]. In all 3 workflows, likelihood ratio tests were applied using '~ Subject + Visit' as the full model design and '~ Subject' as the reduced model in order to detect genes that were differentially expressed after *A. soehngenii L2-7* infusion compared to after placebo infusion. All p-values were adjusted for multiple comparisons using the Benjamini-Hochberg method[13]. Significance thresholds were 0.05 for sleuth and edgeR and 0.10 for DESeq2. Only genes found to be differentially expressed by all 3 workflows were examined in downstream analyses.

Real Time quantitative polymerase chain reaction (RT-qPCR)

Total RNA was extracted from frozen duodenal biopsies from 12 patients as described above. Briefly, 1μg of RNA was converted to cDNA with iScript cDNA synthesis kit (BioRad, Veenendaal, The Netherlands). qPCR was performed on a ViiA7 PCR machine (Applied Biosystems, Bleiswijk, The Netherlands). using Sybr Green Fast (Bioline Meridian Bioscience, Cincinnati, Ohio, USA). Gene expression was normalized towards the housekeeping gene Actin, and relative gene expression was calculated with the "delta delta Ct" method and shown as 2ˆ-delta delta Ct. Primer sequences are outlined in Supplementary Table 2; all primers were manufactured by Sigma-Aldrich (Zwijndrecht, The Netherlands).

Western blotting

Duodenal biopsies (from 8/9 patients) were lysated in RIPA buffer (Thermo Fisher Scientific, Breda, The Netherlands) containing protease and phosphatase inhibitors (cOmplete™ Protease inhibitor and PhosSTOP Phosphatase Inhibitor Cocktails, Sigma, Zwijndrecht, The Netherlands) using a ceramic beads homogenizer. For westernblotting of cell lysates, Caco-2 cells were incubated for 30 minutes 4˚C in RIPA buffer supplemented with protease and phosphatase inhibitors. BCA protein assay kit (Thermo Fisher) was used to determine protein concentrations.β-mercaptoethanol was added as reducing agent to all sample lysates, which were run on 4-12% polyacrylamide gels (BioRad, GE, Boston, USA) in MES running buffer. Proteins were transferred to PVDF membranes (BioRad) and were blocked using 5% milk in TBS-T (Tris Buffered Saline – Tween-20). Membranes were incubated

overnight a 4˚C with primary polyclonal rabbit antibodies anti-Reg1B (for Figure 6A/6G: 1:500, E-AB-52897, Elabscience, Houston, USA) and Actin (AB306371, Abcam, Cambridge, UK) or anti –Reg1A (for Figure S5G: 1:500, orb100720, Biorbyt, Cambridge, UK). Horseradish peroxidase (HRP)-conjugated secondary antibodies (R&D systems, Minneapolis, USA) were incubated for 1hour at room temperature. HRP activity was visualized with peroxidase substrate for enhanced chemiluminescence and imaged with ChemiDoc MP Imaging System (BioRad) using Image Lab software (BioRad). Densitometric quantification analysis was performed using the Image J software. All protein levels were normalized to the loading control (β-actin). Reg1B protein expression shown as ratio of densitometric quantification of Reg1B versus β-actin and as intraindividual fold-changes of treatment versus placebo (expression rates of placebo group normalized to mean to represent distribution in expression levels among subjects). In order to show lack of cross-reactivity of the antibodies anti-Reg1B and anti-Reg1A, recombinant Reg1A (Prospec) and Reg1B (Sino Biological) proteins were loaded on polyacrylamide gels and immunoblotted using antibodies anti-Reg1A (orb100720, Biorbyt) or Reg1B (E-AB-52897, Elabscience) (Figure S5I,K).

Immunohistochemical staining

Formalin-fixed paraffin-embedded (FFPE) duodenal 4 μm sections were utilized for immunohistochemical staining. Slides were deparaffinized in 100% Xylene and rehydrated in ethanol (100%, 96% and 70%) and H2O, following by block of endogenous peroxidase in 3% H2O2 methanol for 20 minutes and heat-induced epitope retrieval (HIER) in citrate buffer pH 6.0 at 98°C for 10 minutes in the Thermo Scientific PT Module. After incubation for 10 minutes with Ultravision protein block (Thermo Fisher Scientific, Breda, The Netherlands), FFPE sections were incubated with anti-Reg1B primary antibody (for Figure 6D,E: 1:100 dilution in TBS, MA5-29517, Invitrogen, Waltham, Massachusetts, USA) for 1 hour at room temperature (RT), following by incubation with the secondary antibodies BrightVision Poly-HRP-conjugates goat anti-rabbit IgG (undiluted) for 30 minutes. For assessing the expression and localization of Reg1B in duodenal tissue with different antibodies and to compare its expression to the one of Reg1A (Figure S5H), following 10-minutes HIER in citrate buffer, duodenal sections were incubated with primary antibodies against Reg1B (1:2000, E-AB-52897, Elabscience, Houston, USA) or against Reg1A (1:2000, orb100720, Biorbyt, Cambridge, UK). All single-stainings were visualized with 3,3'Diaminobenzidine (DAB) kit (Sigma Aldrich, Zwijndrecht, The Nederlands).

For the triple staining of REG1B, lysozyme and mucin were stained in sequential order using sequentially cut duodenal FFPE sections. Reg1B expression was visualized by: 10-minute HIER in citrate buffer pH 6.0 at 98°C, 1-hour incubation at RT with anti-Reg1B rabbit IgG (Invitrogen, MA5-29517, 1:100 dilution in TBS), 30-minute incubation with BrightVision Poly-alkaline phosphatase (AP)-conjugated goat anti-rabbit IgG (undiluted) and staining development with Perma Red/AP kit (Diagnostic BioSystem, Pleasanton, California, USA). Lysozyme (as marker of Paneth cells) was stained

following: 5-minute HIER in Tris-EDTA pH 9.0 buffer at 98°C, 30-minute incubation at RT with polyclonal rabbit anti-lysozyme (1:2000 dilution in TBS, Dako EC 3.2.1.17, Agilent Technologies, Santa Clara, California, USA), 30-minute incubation with BrightVision Poly-HRP-conjugated goat anti-rabbit IgG (1:2 dilution in TBS) and staining development with Perma Yellow/HRP kit (Diagnostic BioSystem). For the final detection of acidic mucins (to mark Goblet cells), FFPE double-stained slides were incubated with Alcian Blue solution (1% in 3% acetic acid, pH 2.5, Sigma Aldrich) for 5 minutes and eventually covered with coverslips using VectaMount mounting medium (Thermo Fisher Scientific, H-5000).

Cell culture and assay procedure

Caco-2 cells were cultured in Gibco Dulbecco's Modified Eagle Medium (DMEM) supplemented with 10% fetal bovine serum (FBS), 100 IU/ml penicillin, 100 IU/ml streptomycin, and 2mM glutamine (Thermo Fisher Scientific) in T75 flasks. The day prior to the stimulation assays, cells were seeded at $1x10^5$/well in a 12-well plates; after resting overnight, cells were exposed to 1mM butyrate or 1 µg/ml muramyl dipeptide (MDP) (both stock solutions diluted in water) for 6 hours. Afterwards cells were washed once in PBS and lysated in RIPA buffer. Reg1B concentrations were determined by ELISA (Cloud-Clone Corp., Uscn Life Science Kit Inc., Wuhan, China) accordingly to the manufacturer's instructions in Caco-2 cells exposed to increasing concentrations of *A. soehngenii* L2-7 cells (10^5/ml and 10^6/ml). Prior to use in cell culture, bacteria were heat-inactivated at 65°C for 20 minutes. BCA protein assay kit (Thermo Fisher) was used to assess protein concentrations.

Measurements of fecal SCFA and plasma SCFA, incretins, bile acids and Reg1B

Fecal SCFAs (butyrate, acetate, propionate) were measured in morning stool samples (N=11), directly frozen at -20°C after collection, using gas chromatography coupled to tandem mass spectrometry detection (GC-MS/MS) as described previously[14]. Briefly, approximately 20-100 mg of fecal samples were mixed with internal standards, added to glass vials and freeze dried. All samples were then acidified with HCl, and SCFAs were extracted with two rounds of diethyl ether extraction. The organic supernatant was collected, the derivatization agent N-tert-butyldimethylsilyl-N-methyltrifluoroacetamide (Sigma-Aldrich, Stockholm, Sweden) was added and samples were incubated at room temperature overnight. SCFAs were quantified with a gas chromatograph (Agilent Technologies 7890A, Santa Clara, California, USA) coupled to a mass spectrometer (Agilent Technologies 5975C). Short chain fatty acid standards were attained from Sigma-Aldrich (Stockholm, Sweden).

Plasma SCFA (butyrate, acetate, propionate) were measured at Cleveland Clinic (OH, USA) in heparin plasma samples (N=12), directly frozen at -80-°C after collection, using gas chromatography coupled to TANDEM mass spectrometry (GC-MS/MS) as previously described[15]. Briefly, 30 µl aliquots of plasma were mixed with 50 µl 2-Butanol/Pyridine (3:2) and 5 µl containing the heavy labeled internal

standards. Afterwards, the carboxylic acids were derivatized by mixing 50 µl supernatant with 10 µl isobutyl chloroformate, followed by vortexing and sonicating the mixture. After derivatization, 50 µl hexane were added and mixed; following centrifugation, the top hexane layer was removed for GC-MS/MS analysis and 1 µl was injected into GC column. The quantitation of butyric acid, acetic acid, and propionic acid was performed using isotope dilution GC-MS/MS and the absolute concentration of each SCFA was determined using calibrations curves measured for each analyte. Samples were analyzed on a Thermo TSQ-Evo triple quadrupole mass spectrometer interfaced with the Trace 1310 gas chromatograph (Thermo Fisher Scientific). Chromatographic separation was achieved by using an HP-5MS fused-silica capillary column (30 m × 0.250 mm × 0.25 µm; Agilent Technologies, Santa Clara, CA, USA) coated with 5% phenymethyl siloxane as previously described[15]. The mass spectrometer was used in MRM mode with the following parent to daughter ion transitions: m/z 61.0 → 43.0 for acetic acid, m/z 63.0 → 45.0 for [13C2]-acetic acid, m/z 61.0 → 43.0 m/z 71.0 → 41.0 for butyric acid, m/z 78.1 → 46.1 for D7-butyric acid, m/z 75.1 → 57.0 for propionic acid, m/z 77.1 → 59.0 for D2-propionic acid.

Plasma incretin levels of all 12 individuals were determined in postprandial (2-hour mixed meal test) samples as previously described[16]. Plasma concentrations of GIP (total) and GLP-1 (total) were measured by Holst group with ELISA (cat no. 10-1258-01 and 10-1278-01, Mercodia, Sweden). All quality controls provided by the manufacturer were within allowed limits. All samples from the same individual were measured in the same assay run.

Concentrations of the secondary bile acids tauro-omega-muricholic acid (TOMCA), tauroursodeoxycholic acid (TUDCA), taurodeoxycholic acid (TDCA), tauroursodeoxycholic acid (TUDCA), taurolithocholic acid (TLCA), glycohyodeoxycholic acid (GHDCA), glycodeoxycholic acid (GDCA), glycoursodeoxycholic acid (GUDCA), glycolithocholic acid (GLCA), omega-muricholic acid (OMCA), deoxycholic acid (DCA), ursodeoxycholic acid (UDCA), lithocholic acid (LCA), hyodeoxycholic acid (HDCA), murocholic acid (MuroCA), iso-ursodeoxycholic acid (IsoUDCA) were measured in plasma samples from all 12 participants by means of ultra-performance liquid chromatography-tandem mass spectrometry (UPLCMS/MS), as previously performed[17]. Briefly, samples (50µl) were extracted with 10 volumes of methanol containing deuterated internal standards (d_4-TCA, d_4-GCA, d_4-GCDCA, d_4-GUDCA, d_4-GLCA, d_4-UDCA, d_4-CDCA, d_4-LCA; 50nM of each). After 10 minutes of vortex and 10 minutes of centrifugation at 20 000g, the supernatant was evaporated under a stream of nitrogen and reconstituted in 200µl methanol:water [1:1]. The samples were injected (5µl) and bile acids were separated on a C18 column (1.7µ, 2.1 x 100mm; Kinetex, Phenomenex, USA) using water with 7.5mM ammonium acetate and 0.019% formic acid (mobile phase A) and acetonitrile with 0.1% formic acid (mobile phase B). The chromatographic separation started with 1 minute isocratic separation at 20%B. The B-phase was then increased to 35% during 4 minutes. During the next 10 minutes the B-phase was increased to 100%. The B-phase was held at 100% for 3.5 minutes before

returning to 20%. The total runtime was 20 minutes. Bile acids were detected using multiple reaction monitoring (MRM) in negative mode on a QTRAP 5500 mass spectrometer (Sciex, Concord, Canada) and quantification was made using external standard curves.

Concentrations of Reg1B in plasma samples and duodenal tissue lysates was assessed by ELISA (Cloud-Clone Corp., Uscn Life Science Kit Inc., Wuhan, China) accordingly to the manufacturer's instructions.

Strain-specific qPCR

The DNA concentrations were determined fluorometrically (Qubit dsDNA HS assay; Invitrogen) and adjusted to 1 ng/µl prior to use as the template in qPCR. Primers targeting 16S rRNA gene of *A. soehngenii* L2-7 EhalF (5'GCGTAGGTGGCAGTGCAA) and EhalR (5'GCACCGRAGCCTATACGG) (Ramirez et al. 2008) were used for quantification. Standard template DNA was prepared from the 16S rRNA gene of *A. soehngenii* L2-7 by amplification with primers 27F (5'-AGAGTTTGATCCTGGCTCAG-3') and 1492R (5'-GGTTACCTTGTTACGACTT-3'). Standard curves were prepared with nine standard concentrations of 100 to 10^8 gene copies/µl. PCRs were performed in triplicate with iQ SYBR Green Supermix (Bio-Rad) in a total volume of 10 µl with primers at 500 nM in 384-well plates sealed with optical sealing tape. Amplification was performed with an iCycler (Bio-Rad, USA) with the following protocol: one cycle of 95°C for 10 min; 40 cycles of 95°C for 15 s, 55°C for 20 s, and 72°C for 30 s each; one cycle of 95°C for 1 min, one cycle of 60°C for 1 min, and a stepwise increase of the temperature from 60 to 95°C (at 0.5°C per 5 s) to obtain melt curve data. Data were analysed using the Bio-Rad CFX Manager 3.0.

Fecal 16S rRNA gene amplicon sequencing and bioinformatics

DNA extraction from fecal samples from 11 patients was performed using the repeated bead beating protocol as previously described[18]. DNA was eluted in 50 µl of DNAse- RNAse-free water and its concentration and quality were evaluated using NanoDrop 2000 spectrophotometry. Subsequently, DNA was diluted to reach a concentration of 20 ng/µl which served as template for PCR. The V5-V6 region of 16S ribosomal RNA (rRNA) gene was amplified in duplicate PCR reactions for each sample in a total reaction volume of 50 µl using a master mix containing 1 µl of a unique barcoded primer, 784F-n and 1064R-n (10 µM each per reaction), 1 µl dNTPs mixture, 0.5 µl Phusion Green Hot Start II High-Fidelity DNA Polymerase (2 U/µl; Thermo Scientific, Landsmeer, The Netherlands), 10 µl 5× Phusion Green HF Buffer, and 36.5 µl DNAse- RNAse-free water[19]. The amplification program included 30 seconds (s) of initial denaturation step at 98°C, followed by 25 cycles of denaturation at 98°C for 10 s, annealing at 42°C for 10 s, elongation at 72°C for 10 s, and a final extension step at 72°C for 7 minutes. The PCR product was visualized on 1% agarose gel (~280 bp) and purified with CleanPCR kit (CleanNA, Alphen aan den Rijn, The Netherlands). The concentration of the purified PCR product was measured with Qubit dsDNA BR Assay Kit (Invitrogen, California, USA) and 200 ng of microbial

DNA from each sample were pooled for the creation of the final amplicon library which was sequenced (150 bp, paired-end) on the Illumina HiSeq 2500 platform (GATC Biotech, Constance, Germany).

Raw reads were demultiplexed using the Je software suite (v2.0)[20] allowing no mismatches in the barcodes. After removing the barcodes, linker and primers, reads were mapped against the human genome using bowtie2 (v2.4.1)[21] in order to remove human reads. Surviving microbial forward and reverse reads were pipelined separately using DADA2 (v1.12.1)[22]. Amplicon Sequence Variants (AVSs) inferred from the reverse reads were reverse-complemented and matched against ASVs inferred from the forwards reads. Only non-chimeric forward reads ASVs that matched reverse-complemented reverse reads ASVs were kept. ASV sample counts were inferred from the forward reads. ASV taxonomy was assigned using DADA2 and the SILVA (v132) database. The resulting ASV table and taxonomy assignments were integrated using the phyloseq R package (v1.28.0)[23]. ASVs sequences were aligned using MAFFT (v.7.427)[24] using the auto settings. A phylogenetic tree was constructed from the resulting multiple sequence alignment with FastTree (v.2.1.11 Double Precision)[25] using a generalized time-reversible model ('-gtr'). Biopsy samples were rarefied to 24947 counts per sample, while fecal samples were rarefied to 13229 counts per sample. The vegan R package (v2.5.6)[26] was used to calculate alpha-diversity metrics (Shannon index and ASV richness) and Bray-Curtis dissimilarities. Weighted-Unifrac distances were calculated using the phyloseq package.

Power calculation and statistical analyses

We based our power calculation on the study of Van Baarlen *et al.*[27], in which a striking difference in duodenal mucosal transcriptomic profiling was reported 6 hours after introduction of a single *Lactobacillus* bacterial strain. Based on 60% decrease in duodenal *Fxr* gene expression upon *A. soehngenii* L2-7 administration to db/db mice, compared to placebo[18], with one sample Chi^2 test, the sample size in each group needed to be 12 in order to have a group proportion of 0.5 and with a comparison proportion of 0.1. Mean absolute deviation of glucose (MAD), continuously measured using FreeStyle Libre technology, was calculated using the default 'mad' function from R stats package[28]. Wilcoxon signed rank tests and Mann-Whitney U-tests were used to compare within-group changes of related samples and to compare intervention groups. Student's t-test was used for analyzing differences in groups from *in vitro* experiments. Area under the curve (AUCs) for MMT measurement were calculated using the DescTools package (v0.99.36) [29,30]. Correlation plots were made using the corrplot package (v0.84) [31]. The mixOmics package (v6.12.1) [32] was used to perform multilevel PCA analyses. Principal Coordinate Analyses (PCoA) were performed using the ape package (v5.4)[33]. All other statistical analyses and visualizations were performed in R (v4.0.1)[34] using the tidyverse (v1.3.0)[35] and ggplot2 package (v3.3.1)[30]. P values <0.05 were considered statistically significant.

SI References

1. Gilijamse, P. W. *et al.* Treatment with Anaerobutyricum soehngenii: a pilot study of safety and dose–response effects on glucose metabolism in human subjects with metabolic syndrome. *npj Biofilms Microbiomes* **6**, 1–10 (2020).

2. Andrews, S. FastQC: a quality control tool for high throughput sequence data. (2015).

3. Bolger, A. M., Lohse, M. & Usadel, B. Trimmomatic: a flexible trimmer for Illumina sequence data. *Bioinformatics* **30**, 2114–2120 (2014).

4. Bray, N. L., Pimentel, H., Melsted, P. & Pachter, L. Near-optimal probabilistic RNA-seq quantification. *Nat. Biotechnol.* **34**, 525–527 (2016).

5. Pimentel, H., Bray, N. L., Puente, S., Melsted, P. & Pachter, L. Differential analysis of RNA-seq incorporating quantification uncertainty. *Nat. Methods* **14**, 687–690 (2017).

6. Love, M. I., Huber, W. & Anders, S. Moderated estimation of fold change and dispersion for RNA-seq data with DESeq2. *Genome Biol.* **15**, 550 (2014).

7. Robinson, M. D., McCarthy, D. J. & Smyth, G. K. edgeR: a Bioconductor package for differential expression analysis of digital gene expression data. *Bioinformatics* **26**, 139–140 (2010).

8. Robinson, M., Mccarthy, D., Chen, Y., Lun, A. & Smyth, G. K. edgeR: differential expression analysis of digital gene expression data. (2012).

9. Fernandes, A. D. *et al.* Unifying the analysis of high-throughput sequencing datasets: characterizing RNA-seq, 16S rRNA gene sequencing and selective growth experiments by compositional data analysis. *Microbiome* **2**, 15 (2014).

10. McCarthy, D. J., Chen, Y. & Smyth, G. K. Differential expression analysis of multifactor RNA-Seq experiments with respect to biological variation. *Nucleic Acids Res.* **40**, 4288–4297 (2012).

11. Soneson, C., Love, M. I. & Robinson, M. D. Differential analyses for RNA-seq: transcript-level estimates improve gene-level inferences. *F1000Research* **4**, 1521 (2015).

12. Durinck, S., Spellman, P. T., Birney, E. & Huber, W. Mapping identifiers for the integration of genomic datasets with the R/Bioconductor package biomaRt. *Nat. Protoc.* **4**, 1184 (2009).

13. Benjamini, Y. & Hochberg, Y. Controlling the false discovery rate: a practical and powerful approach to multiple testing. *J. R. Stat. Soc. Ser. B* 289–300 (1995).

14. Wichmann, A. *et al.* Microbial modulation of energy availability in the colon regulates intestinal transit. *Cell Host Microbe* **14**, 582–590 (2013).

15. Arnon D Lieber, AD. et al. Loss of HDAC6 alters gut microbiota and worsens obesity. FASEB J 33(1), 1098-1109 (2019).

16. Kootte, R. S. *et al.* Improvement of Insulin Sensitivity after Lean Donor Feces in Metabolic Syndrome Is Driven by Baseline Intestinal Microbiota Composition. *Cell Metab.* (2017). doi:10.1016/j.cmet.2017.09.008

17. Tremaroli, V. *et al.* Roux-en-Y Gastric Bypass and Vertical Banded Gastroplasty Induce Long-Term Changes on the Human Gut Microbiome Contributing to Fat Mass Regulation. *Cell Metab.* **22**, 228–238 (2015).

18. Salonen, A. *et al.* Comparative analysis of fecal DNA extraction methods with phylogenetic microarray: Effective recovery of bacterial and archaeal DNA using mechanical cell lysis. *J.*

Microbiol. Methods **81**, 127–134 (2010).

19. Ramiro-Garcia, J. *et al.* NG-Tax, a highly accurate and validated pipeline for analysis of 16S rRNA amplicons from complex biomes. *F1000Research* **5**, 1791 (2016).

20. Girardot, C., Scholtalbers, J., Sauer, S., Su, S.-Y. & Furlong, E. E. M. Je, a versatile suite to handle multiplexed NGS libraries with unique molecular identifiers. *BMC Bioinformatics* **17**, 419 (2016).

21. Langmead, B. & Salzberg, S. L. Fast gapped-read alignment with Bowtie 2. *Nat. Methods* **9**, 357 (2012).

22. Callahan, B. J. *et al.* DADA2: High-resolution sample inference from Illumina amplicon data. *Nat Meth* **13**, 581–583 (2016).

23. McMurdie, P. J. & Holmes, S. phyloseq: An R Package for Reproducible Interactive Analysis and Graphics of Microbiome Census Data. *PLoS One* **8**, e61217 (2013).

24. Katoh, K., Misawa, K., Kuma, K. & Miyata, T. MAFFT: a novel method for rapid multiple sequence alignment based on fast Fourier transform. *Nucleic Acids Res.* **30**, 3059–66 (2002).

25. Price, M. N., Dehal, P. S. & Arkin, A. P. FastTree 2 - Approximately maximum-likelihood trees for large alignments. *PLoS One* **5**, e9490 (2010).

26. Oksanen, J. *et al.* vegan: Community Ecology Package. (2017).

27. van Baarlen, P. *et al.* Differential NF- B pathways induction by Lactobacillus plantarum in the duodenum of healthy humans correlating with immune tolerance. *Proc. Natl. Acad. Sci.* **106**, 2371–2376 (2009).

28. Fokkert, M. J. *et al.* Performance of the freestyle libre flash glucose monitoring system in patients with type 1 and 2 diabetes mellitus. *BMJ Open Diabetes Res. Care* **5**, 1–8 (2017).

29. Signorell, A. DescTools: Tools for Descriptive Statistics. (2020).

30. Wickham, H. *ggplot2: Elegant Graphics for Data Analysis*. (Springer-Verlag New York, 2016).

31. Wei, T. & Simko, V. R package 'corrplot': visualization of a correlation matrix (version 0.84).'. *Retrived from https//github. com/taiyun/corrplot* (2017).

32. Cao, K.-A. Le, Rohart, F., Gonzalez, I. & Dejean, S. mixOmics: Omics Data Integration Project, package version 6.1.2 https://CRAN.R-project.org/package=mixOmics. (2017).

33. Paradis, E. & Schliep, K. ape 5.0: an environment for modern phylogenetics and evolutionary analyses in R. *Bioinformatics* **35**, 526–528 (2019).

34. R Core Team. R: A language and environment for statistical computing. R Foundation for Statistical Computing. (2016).

35. Wickham, H. *et al.* Welcome to the Tidyverse. *J. Open Source Softw.* **4**, 1686 (2019).

SI Legends of Figures and Tables

Figure S1: Fecal *A. soehngenii* L2-7 levels

Fecal *A. soehngenii* L2-7 levels determined by qPCR at 0, 24 hours, 1 week, 2 weeks after placebo/treatment-interventions. Values indicate gene copies per gr of feces.

Figure S2: Fecal short-chain fatty acids

(A) Concentrations (nmol/mg dried feces weight) of butyrate, (**B**) acetate, and (**C**) propionate in morning stool samples obtained at baseline and 1 day after placebo/treatment-intervention.

Figure S3: Postprandial glucose and insulin
(**A**) Plasma glucose levels (mmol/l) at 0, 20, 30, 120 minutes during mixed meal test (MMT). (**B**) Plasma glucose levels during MMT as total area under the curve (AUC). (**C**) Plasma insulin levels (pmol/l) at 0, 20, 30, 120 minutes during MMT. (**D**) Plasma insulin levels during MMT as total area under the curve (AUC).

Figure S4: Plasma short-chain fatty acids

(A) Concentrations (μM) of butyrate, (**B**) acetate, and (**C**) propionate in plasma at 120 minutes of mixed meal test (MMT).

Figure S5: Duodenal expression of REG genes and Reg1A/1B proteins

Gene expression measured by qPCR in duodenal biopsies at 6 hours post-intervention of (**A**) *REG1B* (different set of forward and reverse primers than in Figure 6B), (**B**) *REG3A*, (**C**) *REG3G*, and (**D**) *REG4*. (**A-D**) Data showing the relative gene expression (to placebo) using the 2ˆ-(delta delta Ct) method. (**E**) Quantification of Reg1A expression levels in duodenal biopsies, Reg1A expression normalized to β-actin (loading control). (**F**) Reg1A expression shown as fold-change treatment versus placebo. (**G**) Westernblot images of duodenal lysates blotted with antibodies against Reg1A and β-actin. (**H**) Immunohistochemical staining of Reg1B (different antibodies used than in Figures 6D,6E) and Reg1A in duodenal biopsies. (**I,K**) Westernblot images showing the specificity of the antibodies against Reg1B and Reg1A; (**I**) Westernblotting for Reg1B: enhanced band intensity with increasing amount of loaded recombinant human (rh)Reg1B and absence of a band when rh Reg1A is loaded; ; (**K**) Westernblotting for Reg1A: stronger band intensity with increasing amount of loaded rh Reg1A and absence of a band when rh Reg1B is loaded. (**J**) Circulating levels (ng/ml) of Reg1B measured by ELISA in plasma samples taken at 8 hours post-intervention. (**L**) Reg1b expression by Caco-2 cells in response to exposure to increasing concentrations of heat-inactivated *A. soehngenii* L2-7 cells.

Figure S6: Assessment of carry-over affect between week 0 and week 4

(**A**) Fecal *A. soehngenii* L2-7 levels determined by qPCR at baseline (week 0 and week 4); values indicate gene copies per gr of feces. (**B**) Concentrations (nmol/mg dried feces weight) of butyrate in morning stool samples obtained at baseline (week 0 and week 4). (**C**) Plasma GLP-1 levels during mixed meal test (MMT) shown as total area under the curve (AUC). (**D**) Median absolute deviation (MAD) of continuous glucose measurements (CGM) over the first 24 hours after placebo/treatment-intervention.

Table S1: Baseline characteristics and safety parameters at both study visits

Data expressed as medians and interquartile ranges. There were no differences after the *A. Soehngenii* L2-7 infusion compared to the placebo infusion. BMI: body mass index, HOMA-IR: homeostatic model assessment of insulin resistance, HbA1c: glycated hemoglobin, HDL: high-density lipoprotein, LDL: low-density lipoprotein; AST: aspartate transaminase, ALT: alanine transaminase, AP: alkaline phosphatase; γgt: gamma-glutamyltransferase; CRP: c-reactive protein.

Table S2

Primer sequences utilized in the analysis of duodenal gene expression. *: primers used in Figure S5A.

Koopen A, *et al. Gut* 2021;0:1–11. doi: 10.1136/gutjnl-2020-323297

Table S1

	Placebo	A. Soehngenii	P - value
Weight (kg)	110.1 [100.0 – 120.2]	110.4 [101.3 – 122.0]	0.812
BMI (kg/m2)	33.4 [32.2 – 38.]	33.7 [31.8 – 37.8]	0.859
Blood pressure: systolic (mmHg)	135 [129 – 147]	144 [131 – 156]	0.258
Blood pressure: diastolic (mmHg)	89 [84 – 91)	91 [79 – 95)	0.917
Fasting glucose (mmol/L)	5.3 [5.0 – 5.6]	5.1 [4.8 – 5.7]	0.430
Insulin (pmol/L)	65 [48 – 83]	56 [34 – 81]	0.099
HOMA - IR	2.3 [1.7 – 2.8]	1.9 [1.1 – 2.8]	0.158
HbA1c (mmol/mol)	37 [36 – 39]	37 [36 – 39]	0.942
Cholesterol: total (mmol/L)	5.29 [4.57 – 6.26]	5.13 [4.71 – 6.08]	0.255
Cholesterol: HDL (mmol/L)	1.17 [0.91 – 1.31]	1.13 [0.97 – 1.32]	0.929
Cholesterol: LDL (mmol/L)	3.05 [2.69 - 3.90]	3.21 [2.79 – 3.83]	0.638
Cholesterol: triglycerides (mmol/L)	1.65 [1.12 – 2.92]	1.66 [1.19 – 2.31]	0.433
Creatinine (umol/L)	87 [78 – 92]	84 [79 – 93]	0.342
AST (U/L)	25 [19 – 31]	26 [23 – 33]	0.109
ALT (U/L)	25 [21 – 36]	27 [22 – 35]	0.124
AP (U/L)	70 [62 – 85]	72 [60 -87]	0.783
yGT (U/L)	39 [26 – 52]	31 [26 – 49]	0.254
CRP (mg/ml)	2.8 [1.8 – 5.0]	3.0 [2.3 – 5.3]	0.477
Leukocytes (10^e9/L)	6.2 [5.6 – 6.7]	6.5 [5.9 – 7.3]	0.130
Caloric intake (kcal/day)	1843 [1607 – 2090]	1888 [1667 – 2041]	0.424
Fat intake (g)	68 [57 – 75]	61 [56 – 81]	0.790
Protein intake (g)	76 [65 – 85]	77 [60 – 91]	0.333
Carbohydrate intake (g)	201 [162 – 233]	228 [173 – 254]	0.241
Fiber intake (g)	18 [14 – 19]	19 [16 – 21]	0.339

Koopen A, *et al. Gut* 2021;0:1–11. doi: 10.1136/gutjnl-2020-323297

Table S2

Gene	Forward primer sequence	Reverse primer sequence
GPR43/FFAR2	TGCTACGAGAACTTCACCGAT	GGAGAGCATGATCCACACAAAAC
TGR5	CACTGTTGTCCCTCCTCTCC	ACACTGCTTTGGCTGCTTG
FXR	TACATGCGAAGAAAGTGTCAAGA	ACTGTCTTCATTCACGGTCTGAT
FGF19	CGGAGGAAGACTGTGCTTTCG	CTCGGATCGGTACACATTGTAG
OSTalpha	CTGGGCTCCATTGCCATCTT	CACGGCATAAAACGAGGTGAT
REG1B	GGTCCCTGGTCTCCTACAAG	TCCATTTCTTGAATCCTGAGCA
REG1A	GGTCCCTGGTCTCCTACAAG	CATTTCTGGAATCCTGTGCTTG
REG1B*	AGTAGTGGGTCCCTGGTCTC	TGAATCCTGAGCATGAAGTCA
REG3A	AGCTACTCATACGTCTGGATTGG	CACCTCAGAAATGCTGTGCTT
REG3G	GGTGAGGAGCATTAGTAACAGC	CCAGGGTTTAAGATGGTGGAGG
REG4	CTGCTCCTATTGCTGAGCTG	GGACTTGTGGTAAAACCATCCAG
ACTB	CCAACCGCGAGAAGATGA	CCAGAGGCGTACAGGGATAG